

Calcium Hydroxide as Precipitative Antiscalant for Nanofiltration

A.R. Heinsbroek

Master's Thesis

Master of Science Thesis in Civil Engineering

Calcium Hydroxide Microparticles as Precipitative Antiscalant for Nanofiltration

Author:
A.R. Heinsbroek, BSc.

Committee:
Prof. Dr. ir. L.C. Rietveld
Dr. ir. S.G.J. Heijman
Dr. ir. H.J.M. Kramer
ir. A.H. Haidari

DELFT UNIVERSITY OF TECHNOLOGY

Faculty of Civil Engineering and Geosciences
Department of Water Management
Sanitary Engineering Section

May 6, 2016

*Twenty years from now you will be more disappointed
by the things you didn't do than by the ones you did do.
So throw off the bowlines. Sail away from the safe
harbor. Catch the trade winds in your sails.
Explore. Dream. Discover.*

MARK TWAIN

Preface

The report in front of you is the result of a research performed to finalize my study Civil Engineering at the Delft University of Technology.

For a period of little over a year I've had the pleasure of developing a simple but radical idea into a complete first proof-of-principle. It was a year of continuous ups-and-downs, of successes and setbacks. A year of long hours working in the lab and even longer hours of lying awake at night, while hundreds of meters away my trusty little machine kept on working, tirelessly and autonomously performing (and often botching!) experiments. But also a year of camaraderie with my colleagues, of learning new technologies and skills and most importantly, of enthusiasm and often tremendous fun.

I would like to thank the members of my committee; professor Luuk Rietveld, Herman Kramer, Amir Haidari and especially my day-to-day supervisor Bas Heijman for not only supporting me during my work and providing me with invaluable advice and discussions, but for giving me the freedom and trust to perform my studies the way I did.

In addition, I would like to thank Sander de Vree for his enthusiasm and support in designing and building my lab setup, Armand Middeldorp and Mohammed Jafar for helping out in the lab whenever possible and my colleagues from room 4.54 for providing a great working environment.

Finally I would like to thank my parents for their unconditional support and trust allowing me to reach where I am today, and my sisters, friends and roommates for often providing me with some much needed distraction.

Abel Heinsbroek

Delft, May 2016

Abstract

Nano Filtration (NF) is an advanced treatment process that is able to remove molecules and ions from water using special, synthetic, membrane modules. Under high pressure the so-called feed water enters the membrane module. Part of the water, the permeate, passes through the membrane wall while the rejected ions and molecules are flushed out with the rest of the water, the concentrate.

However, the ratio between product; the permeate, and waste; the concentrate, that can be attained with NF treatment is limited by the concentration of sparingly soluble salts in the feed water. When too much permeate is produced the concentrate stream becomes supersaturated, causing the salts to start precipitating on the membrane surface, a process called *scaling*. The scaling causes an increase in membrane resistance, necessitating a higher pressure, and thus more energy, to treat the same amount of water.

There are several strategies to control scaling in membrane filtration installations such as feed-water alteration and antiscalant dosing, all of which aim to keep the salts dissolved for as long as possible. In this thesis a different approach to prevent scaling is proposed, aiming to promote precipitation instead, albeit in a controlled manner: *precipitative antiscalants*. Instead of precipitating on the membrane wall, the salts precipitate on special particles, which are transported out of the system with the waste stream.

The dosing of calcium hydroxide, $\text{Ca}(\text{OH})_2$, was investigated as precipitative antiscalant for CaCO_3 scaling. $\text{Ca}(\text{OH})_2$ particles exhibit a dissolve-precipitate effect, where CaCO_3 precipitates on the dissolving particles, slowing down further dissolution. This effect is unwanted during application in other processes, but may prove of use as anti scaling mechanism.

To better understand the mechanisms and kinetics involved with $\text{Ca}(\text{OH})_2$ dissolution in carbonate containing solutions a soft-sensor, capable of converting measured pH and EC to total calcium and carbonate, was developed and validated. Using this sensor it was found that, for high dosages of $\text{Ca}(\text{OH})_2$, the formed layer of CaCO_3 was unstable. After a certain length of time the covering layer breaks open, allowing the dissolution reaction to continue at its original rate.

To investigate whether $\text{Ca}(\text{OH})_2$ dosing could function as antiscalant a pilot-plant installation, capable of simulating scaling on a flat-sheet polymeric NF membrane, was constructed. Dosing of $\text{Ca}(\text{OH})_2$ particles in combination with using a feed spacer proved problematic, as the particles got lodged between the spacers and could not be adequately removed. Without a feed spacer installed $\text{Ca}(\text{OH})_2$ dosing as antiscalant was a limited success. With little surface scaling taking place the runtime of the experiment could be extended from a mere 4.5 hours to over 24

hours. Excessive particulate fouling inside the pilot-plant, however, forced the experiment to be halted prematurely.

In the end, although theoretically possible, the problems associated with feed spacers, the necessity of an intermittent cleaning cycle and substantial particulate fouling inside the system make the use of precipitative antiscalants for use with conventional spiral-wound polymeric membranes an unattractive option compared to more traditional anti-scaling measurements.

Contents

Preface	iii
Abstract	v
1 Introduction	1
1.1 Background	1
1.1.1 Membrane Filtration	1
1.1.2 Scaling	1
1.1.3 Scaling Prevention	2
1.1.4 Precipitative Antiscalants	3
1.2 Objective and Research Questions	4
1.3 Research Approach and Report Outline	5
2 Conductivity and pH as a Soft-Sensor for Calcium and Carbonate	7
2.1 Introduction	7
2.1.1 Model Approach	7
2.2 Analytical Solution	9
2.2.1 Chemical Reactions	9
2.2.2 Chemical Balances	9
2.2.3 Activity Coefficients	10
2.2.4 Mass Balances	10
2.3 Numerical Solution	11
2.3.1 Specific Conductivity	11
2.3.2 Newton-Rhaphson's method	13
2.4 Model Validation	14
2.4.1 Method	14
2.4.2 Results	14
3 The Kinetics of Calcium Hydroxide Dissolution in Carbonate Containing Water	17
3.1 Introduction	17
3.1.1 Dissolution in Pure Water	17
3.1.2 Dissolution in Carbonate Containing Water	18
3.2 Materials and Methods	20
3.2.1 Batch Experiments	20
3.3 Results and Discussion	22
3.3.1 Effect of Lime Dissolution and CaCO ₃ Formation on the EC and pH	22
3.3.2 Dissolution Kinetics of Calcium Hydroxide in Carbonate Containing Water	24

4	Calcium Hydroxide as Precipitative Antiscalant for Nanofiltration	31
4.1	Introduction	31
4.2	Materials and Methods	32
4.2.1	Experimental Setup	32
4.2.2	Experimental Procedure	33
4.3	Results and Discussion	38
4.3.1	Pilot-Plant Experiments	38
4.3.2	Particulate Fouling inside the System	39
5	Summary and Conclusions	45
5.1	Soft-Sensor for Total Calcium and Carbonate	45
5.2	Dissolution of Calcium Hydroxide in Carbonate Containing Water	45
5.3	Calcium Hydroxide as Precipitative Antiscalant	46
6	Recommendations	49
A	Analytical Solutions	55
B	Model Source Code	65
C	Calcium IC Measurement Procedure	73
D	Carbonate IC Measurement Procedure	77
E	Flat Sheet Membrane Specifications	79

List of Figures

1.1	Schematic illustration of surface- and bulk crystallization mechanisms.	2
1.2	Precipitative Antiscalants inside a membrane container, having a higher local supersaturation (blue) then the membrane surface.	4
2.1	Flowchart of computation steps taken by the soft-sensor to calculate total calcium and total carbonate from the measured conductivity and pH	8
2.2	Online measured values of Electrical Conductivity (EC) and pH during the validation experiment. The measured values for pH are lagging in the first fifty seconds of the experiment.	15
2.3	Output of the model compared with results from the ion-exchange chromatography analyzer.	15
3.1	Schematic diagram of the Dissolve-Precipitate mechanism (Van Eekeren and van Paassen, 1994)	18
3.2	Photo of the experimental setup used to determine the dissolution kinetics of slaked lime in carbonate containing water.	21
3.3	Surface plots of the influence of the amount of lime dissolved and CaCO_3 precipitated on the electrical conductivity (top) and on the acidity (bottom) of a 4mM CaCl_2 , 8mM NaHCO_3 solution, calculated using the model presented in this chapter. The red lines follow the x-axis (CaCO_3 formed), the green lines follow the y-axis (Ca(OH)_2 dissolved)	23
3.4	Calculated amount of Ca(OH)_2 dissolved over time. The dashed lines indicate the dissolution of Ca(OH)_2 in pure water.	26
3.5	Amount of CaCO_3 precipitated over time	26
3.6	Calculated concentration of total calcium in the solution over time	27
3.7	Calculated concentration of total carbonate in the solution over time	27
3.8	Time of occurrence for the four dissolution phases of the dissolution of 4 mmol Ca(OH)_2 in a 4mM CaCl_2 , 8mM NaHCO_3 solution	28
3.9	Calculated Aquatic speciation distribution over time for the dissolution of 5 mmol Ca(OH)_2 in a 4mM CaCl_2 , 8mM NaHCO_3 solution	28
3.10	Schematization of the dissolve-precipitate-break-collapse mechanism.	29
4.1	Simulated location of the pilot treatment plant, further treating the concentrate of a larger NF treatment plant.	31
4.2	Schematic overview of the experimental setup	36
4.3	Photo of the experimental setup in operation	37

4.4	Photo of the membrane surface before (left) and after (right) backwashing	38
4.5	Photo of the membrane surface before (left) and after (right) completion of experiment 3	40
4.6	Increase of the Membrane Resistance Coefficient (MRC) over time with a 28-mil spacer	41
4.7	Increase of the Membrane Resistance Coefficient (MRC) over time when no spacer is used	41
4.8	Microscope image of the clean membrane surface (top), after experiment 3 (middle) and experiment 4 (bottom).	42
4.9	PID Controller output for the position of the control valve (left) and the variable frequency drive (VFD) output (right) during experiment 4	43
4.10	Accumulation of CaCO ₃ deposits near the inlets of the pressure vessel after conclusion of experiment 4	43

Chapter 1

Introduction

1.1 Background

1.1.1 Membrane Filtration

The use of NF and Reverse Osmosis (RO) treatment for the production of drinking water from surface- and groundwater has been widely studied since the 1980's with an increasing focus on the detection and removal of Organic Micro-Pollutants (OMPs) (Sudhakaran et al., 2013).

Nano Filtration (NF) and Reverse Osmosis (RO) filtration are advanced treatment processes that are able to remove molecules and ions from water using special, synthetic, membrane modules. Under high pressure the so-called *feed water* enters the membrane module. Part of the water, the *permeate*, passes through the membrane wall, whilst the rejected ions and molecules are flushed out with the rest of the water; the *concentrate*.

The ratio between the feed water entering the membrane module and the permeate exiting is called the *recovery*. The permeate production is often expressed as volumetric *flux*; the amount of permeate produced per membrane surface area per hour. The pressure difference between the feed side of the membrane and the permeate, which often exits at atmospheric pressure, is termed the Trans Membrane Pressure (TMP).

NF membranes are generally capable of removing divalent ions such as calcium (Ca^{2+}) and manganese (Mg^{2+}) whereas RO membranes are capable of removing even the smallest monovalent ions such as sodium (Na^+) and chloride (Cl^-). The percentage of ions retained in the concentrate is termed the *retention* (Hendricks, 2010).

1.1.2 Scaling

However, the ratio between product and waste; permeate and concentrate, that can be attained with NF and RO membranes is limited by the concentration of sparingly soluble salts such as Calcite (CaCO_3), Gypsum (CaSO_4) and Barite (BaSO_4) to around sixty to seventy percent (Van de Lisdonk et al., 2001). With increasing recoveries the salts become supersaturated and start to form crystalline deposits which precipitate on the membrane surface, a process called *scaling*.

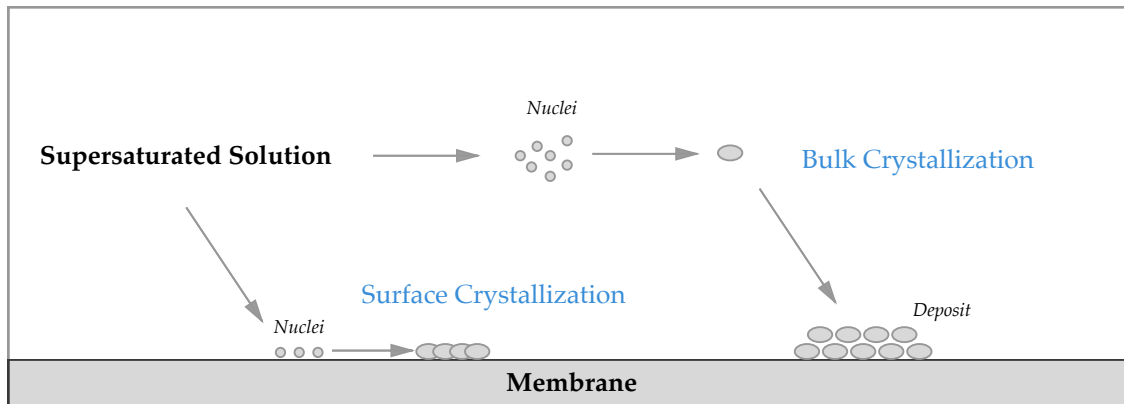


Figure 1.1: Schematic illustration of surface- and bulk crystallization mechanisms.

Three categories of scaling salts can be made; alkaline, non-alkaline and silica based. Compounds commonly found in membrane feed water include calcium carbonate (CaCO_3), calcium sulphate ($\text{CaSO}_4 \cdot x\text{H}_2\text{O}$), barium sulphate (BaSO_4) and silica (SiO_2) (Antony et al., 2011).

Scaling Mechanism

The precipitation of dissolved salts starts with the spontaneous formation of small crystals inside the fluid, a process called *nucleation*. These small crystals rapidly expand as more dissolved salt crystallizes.

Inside a membrane system two forms of crystallization can take place, sometimes simultaneously; *surface-* and *bulk-*crystallization. Surface crystallization is the formation of nucleation sites on the surface of the membrane, which grow laterally to form a covering layer on the membrane surface. For bulk crystallization the nucleation takes place in the supersaturated fluid. The formed particles can settle on the membrane surface, forming loosely adherent deposits (Antony et al., 2011).

Concentration Polarisation

An additional problem that occurs during NF and RO filtration is concentration polarisation. Due to the selective permeability of the membrane, an accumulation of sparingly soluble salts occurs close to the membrane surface. Although concentration polarisation can be limited by using a high crossflow velocity, the increase in concentration near the surface remains around 20 percent (Hendricks, 2010). This results in the highest level of supersaturation to occur near the membrane surface, with precipitation on the surface as a result.

1.1.3 Scaling Prevention

The deposits of scale that form on the membrane surface reduce the membrane's permeability, either by blocking the membrane surface for surface crystallization, or by forming a porous deposit layer through bulk crystallization. Therefore, a higher pressure, and thus more energy,

is required to achieve the same flux. In addition, the frequent chemical cleaning necessary to restore membrane permeability may result in a shorter membrane life expectancy (Van de Lisdonk et al., 2001). Therefore, several mitigation techniques have been developed, which can be grouped into three categories; feed water alteration, operation optimization and system design, and antiscalant addition (Antony et al., 2011).

Feed water alteration is aimed at reducing the formation of scale by increasing the solubility product of the scale forming salts. This can be done either by removing ions using processes such as ion-exchange or pellet-softening, or by reducing the pH of the feed water by dosing acid, which increases the solubility of alkaline scalants such as CaCO_3 .

Changing the system operation or design is another option to keep the risk of scaling at a minimum. The simplest method of preventing scaling is to keep the recovery at a sufficiently low level such that the sparingly soluble salts remain undersaturated. While simple and effective, the resulting increase in concentrate (waste) production is often unacceptable. Another option is the introduction of an intermediate demineralization step between two membrane filtration stages (Bremere et al., 1998; Rahardianto et al., 2007).

The third option is the dosing of specially developed polyelectrolites and polymers called *antiscalants*. These chemicals aim not to remove scale forming compounds, but to hinder and delay the formation and growth of crystals, effectively increasing the solubility limits and therewith enabling a higher recovery (Antony et al., 2011). Because the antiscalant does not generally interact with the scaling ions very low, substoichiometric, dosage levels are required, making them economically attractive to use and limiting their impact on the feed water quality. Antiscalant dosing however has been linked to biofouling problems (Vrouwenvelder et al., 2000) and can result in environmental issues with discharging of the concentrate (Hasson et al., 2011).

1.1.4 Precipitative Antiscalants

A suggested, novel, approach to mitigate the risk of scaling is, instead of trying to prevent scaling from taking place, to promote it, albeit in a controlled manner. By offering the scaling salts a more attractive surface, in the form of microscopic particles, to precipitate on, scaling on the membrane wall may be prevented. The particles transport the scale out of the membrane system with the concentrate stream. A schematization of precipitative antiscalants is presented in figure 1.2.

A somewhat similar process called Membrane Assisted Crystallization (MAC) was explored by TNO (Verdoes, 1996), who used Chemically Enhanced Seeded Precipitation (CESP) in conjunction with traversal flow Micro Filtration (MF) membranes. By dosing microscopically small CaCO_3 seed particles and a base solution a calcium removal efficiency of 98 percent was attained.

Calcium Hydroxide as Combined Softening Chemical and Seed Particle

In their research towards reducing pellet reactor carry-over, Van Eekeren and van Paassen (1994), noted that the dissolution of Ca(OH)_2 particles in carbonate containing water is inhibited by a layer of CaCO_3 forming on the surface of the particle, a process termed the *Dissolve-Precipitate* mechanism.

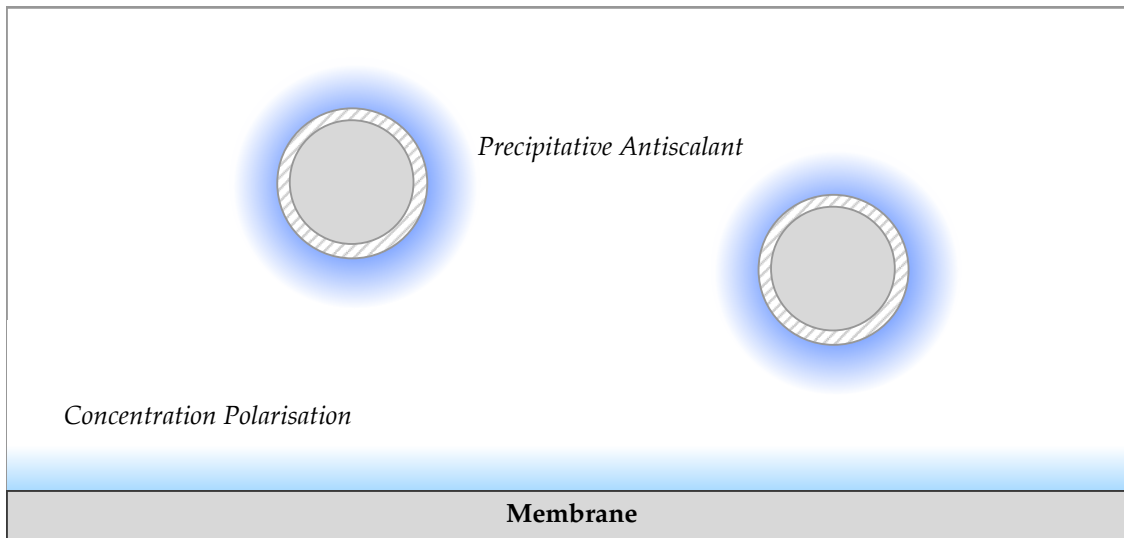


Figure 1.2: Precipitative Antiscalants inside a membrane container, having a higher local supersaturation (blue) than the membrane surface.

This mechanism is unwanted in pellet reactors, where rapid dissolution is necessary for efficient Ca^{2+} removal. It may, however, be of use for scaling prevention in membrane filtration, allowing the $\text{Ca}(\text{OH})_2$ particles to simultaneously act as softening chemical and as precipitation surface. In theory, near the dissolving particle surface, due to diffusion of Ca^{2+} and OH^- ions, the degree of supersaturation of CaCO_3 is highest, resulting in scaling to take place on the particle instead of on the membrane wall.

Advantages of Precipitative Antiscalants

A major advantage of using precipitative antiscalants instead of conventional ones is that the scaling salts are removed from the solution during the treatment process. Rather than staying behind in the solution the salts end up on particles that can be separated from the water and reclaimed.

A specific advantage of using $\text{Ca}(\text{OH})_2$ as antiscalant is that it is a relatively inexpensive chemical commonly used in many other processes (Hendricks, 2010). Additionally, if reclaimed, the CaCO_3 particles can be thermally decomposed back to calcium oxide and calcium hydroxide, effectively creating a closed cycle.

1.2 Objective and Research Questions

The main goal of the research is *“To gain a better understanding into the kinetics of the dissolve–precipitate mechanism and to research the feasibility of using $\text{Ca}(\text{OH})_2$ particle dosing as antiscalating measure for NF filtration.”*

To accurately follow the changes in solution composition during the experiments it is necessary to gain a better understanding of the chemistry involved and to develop a soft–sensor that is

able to calculate solution composition from easily measured Electrical Conductivity (EC) and pH. The first research question therefore becomes:

1. *How can the total concentration of calcium and carbonate in a solution be calculated from the EC and pH?*

A better understanding of the dissolution-mechanisms involved with dissolving $\text{Ca}(\text{OH})_2$ in carbonate containing water is key to investigate the dosing of $\text{Ca}(\text{OH})_2$ particles as precipitative antiscalant. Although several researchers have confirmed the mechanism to occur, little to no knowledge of the changes in solution composition during and after dissolution is available. Therefore the second research question is:

2. *What is the dissolve-precipitate mechanism of slaked lime, how much CaCO_3 can be formed on a particle, how can the process be influenced and what are the kinetics involved?*

An important condition for the application of CESP inside membranes is that the dosed particles either move freely through the membrane and spacer, or can be easily removed by backwashing. This leads to the third research question:

3. *How do the $\text{Ca}(\text{OH})_2$ particles behave inside a spaced NF membrane, do they get lodged between the spacers and if so, can they be easily removed by flushing with air and water?*

Although there are several different scaling salts that can precipitate, to simplify the experiment and to provide a proof-of-concept only CaCO_3 scaling will be evaluated. Therefore the fourth research question is:

4. *Is it possible to prevent CaCO_3 scaling on the membrane surface by adding $\text{Ca}(\text{OH})_2$ particles to the feed water to act as combined seed surface and softening chemical?*

1.3 Research Approach and Report Outline

To attain the goal and to answer the questions mentioned in the previous section the research was performed in three phases.

During the first phase, described in chapter 2, the physical and chemical reactions taking place during $\text{Ca}(\text{OH})_2$ dissolution and CaCO_3 scaling were translated to a soft-sensor for dissolved calcium and carbonate.

In the second phase, described in chapter 3, the kinetics of calcium hydroxide dissolution in carbonate containing water was investigated by means of soft-sensor-supported batch experiments.

In the third phase, described in chapter 4, the possibility of using calcium hydroxide as precipitative antiscalant for nanofiltration was investigated. Several trial experiments were performed using a NF pilot plant.

The objectives and research questions presented in the previous section are answered in chapter 5. Concluding remarks and recommendations for further research are given in chapter 6.

Chapter 2

Conductivity and pH as a Soft-Sensor for Calcium and Carbonate

2.1 Introduction

To gain a better insight into the solution composition during the various experiments conducted during this thesis research a soft-sensor was developed. Soft-Sensors are computational models that can convert relatively easily and continuously measured parameters to a range of other, harder to measure, parameters (Lin et al., 2007).

In this section a soft-sensor is presented that is able to convert two known parameters pH and Electrical Conductivity (EC), both easily and continuously measured using electrodes, to two unknown parameters total calcium T_{Ca} and total carbonate T_{CO} . Although both parameters can be discretely measured by taking samples and using an Ion-Exchange Chromatography (IC) analyzer, the process is very time- and labour-intensive and has a low temporal resolution.

2.1.1 Model Approach

To calculate the total calcium T_{Ca} and total carbonate T_{CO} in a solution a two-step approach is necessary.

First, based on mass-action equations functions for the molarity and activity of all relevant aquatic species, such as $[CaHCO_3^+]$ and $[CO_3^{2-}]$, have to be solved. This system of equations can be solved *analytically* and results in a series of functions in terms of T_{Ca} , T_{CO} , ionic strength I and acidity $[H^+]$.

Due to the ionic strength being dependent on the concentration and charge of the aquatic species, and vice-versa, it is not possible to directly solve T_{Ca} and T_{CO} for a given conductivity and pH. Therefore a second, *numerical*, step, has to be performed to iteratively solve a second system of equations using the functions gained in the previous, analytical, step.

A flowchart of the calculation steps taken by the soft-sensor is presented in figure 2.1.

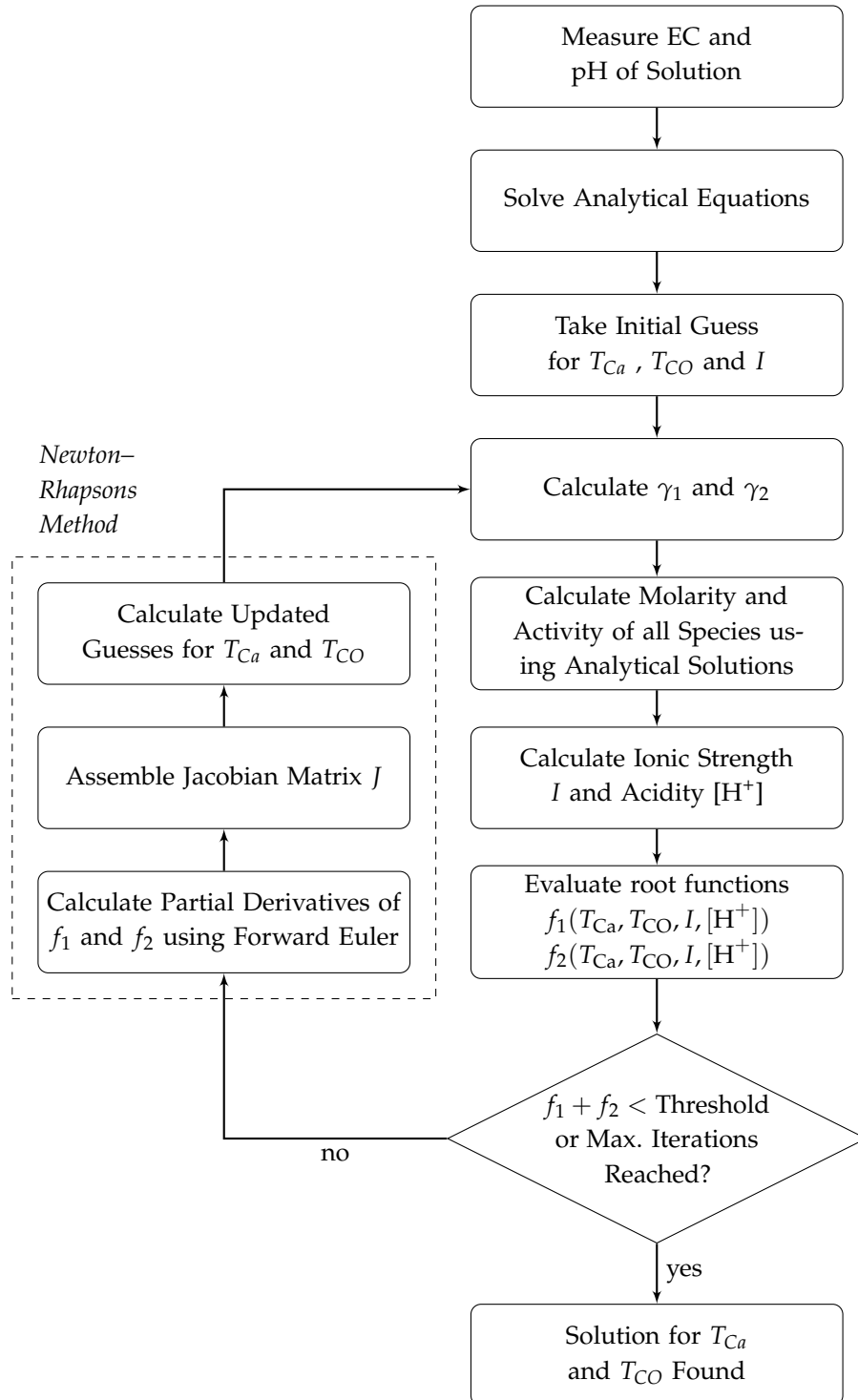
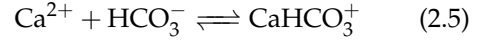
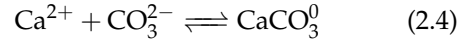
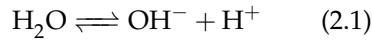


Figure 2.1: Flowchart of computation steps taken by the soft-sensor to calculate total calcium and total carbonate from the measured conductivity and pH

2.2 Analytical Solution

2.2.1 Chemical Reactions

The most prevalent chemical balances occurring in a solution containing calcium and carbonate ions are (Stumm and Morgan, 2012):



In addition to these five main reactions, in solutions of CaCl_2 and NaHCO_3 other interactions between the calcium, sodium, chloride and carbonate ions, such as the formation of NaCO_3^- and CaOH^+ , take place. These interactions however were found, using the PHREEQC model (Parkhurst et al., 1990), to take place at a very limited rate and are therefore, for simplification, ignored in this model.

Note that the calcium carbonate CaCO_3^0 is an ion-pair without charge, and therefore does not represent a solid phase such as calcite, aragonite or vaterite.

2.2.2 Chemical Balances

The chemical reactions occurring can be expressed as mass-action balance equations. By compensating the equilibrium constant for *activity* an expression for the *molality* can be obtained, based on the modified equilibrium constant k_i^* .

$$[\text{H}^+] \cdot [\text{OH}^-] = \frac{k_w}{\gamma_1^2} = k_w^* \quad k_w = 1.00 \cdot 10^{-14} \quad (2.6)$$

$$\frac{[\text{H}^+] \cdot [\text{HCO}_3^-]}{[\text{CO}_2]} = \frac{k_1}{\gamma_1^2} = k_1^* \quad k_1 = 4.44 \cdot 10^{-7} \quad (2.7)$$

$$\frac{[\text{H}^+] \cdot [\text{CO}_3^{2-}]}{[\text{HCO}_3^-]} = \frac{k_2}{\gamma_2} = k_2^* \quad k_2 = 4.69 \cdot 10^{-11} \quad (2.8)$$

$$\frac{[\text{Ca}^{2+}] \cdot [\text{CO}_3^{2-}]}{[\text{CaCO}_3^0]} = \frac{k_3}{\gamma_2^2} = k_3^* \quad k_3 = 6.03 \cdot 10^{-4} \quad (2.9)$$

$$\frac{[\text{Ca}^{2+}] \cdot [\text{HCO}_3^-]}{[\text{CaHCO}_3^+]} = \frac{k_4}{\gamma_2} = k_4^* \quad k_4 = 7.84 \cdot 10^{-2} \quad (2.10)$$

All activity coefficients are obtained from Stumm and Morgan (2012).

2.2.3 Activity Coefficients

The activity coefficients for monovalent ions, γ_1 , and divalent ions, γ_2 , can be calculated from the ionic strength using the Debye-Hückel theory:

$$-\log(\gamma_i) = \frac{A \cdot z_j^2 \sqrt{I}}{1 + B \cdot \alpha^0 \sqrt{I}} \quad (2.11)$$

Where:

$$\begin{array}{l} z_j = \text{Charge number} \\ I = \text{Ionic strength} \\ \alpha^0 = \text{Distance of closest approach} \end{array} \left| \begin{array}{l} [-] \\ [\text{mol} \cdot \text{dm}^{-3}] \\ [\text{m}] \end{array} \right.$$

And (for aquatic solutions with a temperature of 25 °C) $A \approx 0.51 \text{mol}^{-1/2} \text{dm}^{1/2}$ and $B \approx 3.29 \text{nm}^{-1/2} \text{dm}^{-3/2}$ (Hückel, 1923).

An empirical simplification of the Debye-Hückel theory used in this model, discarding the α^0 term, is Davies equation (Davies, 1962):

$$-\log(\gamma_i) = 0.5 \cdot z_j^2 \left(\frac{\sqrt{I}}{1 + \sqrt{I}} - 0.30I \right) \quad (2.12)$$

The ionic strength I of an aquatic solution is the weighted sum of the charge of all ions in that solution:

$$I = \frac{1}{2} \sum_{i=1}^n c_i z_i^2 \quad (2.13)$$

Where:

$$\begin{array}{l} c_i = \text{molarity of species} \\ z_i = \text{charge of species} \end{array} \left| \begin{array}{l} [\text{mol} \cdot \text{dm}^{-3}] \\ [-] \end{array} \right.$$

2.2.4 Mass Balances

To solve the chemical speciation the following mass balances for T_{Ca} and T_{CO} are introduced:

$$T_{Ca} = [\text{Ca}^{2+}] + [\text{CaCO}_3^0] + [\text{CaHCO}_3^+] \quad (2.14)$$

$$T_{CO} = [\text{CO}_2] + [\text{HCO}_3^-] + [\text{CO}_3^{2-}] + [\text{CaCO}_3^0] + [\text{CaHCO}_3^+] \quad (2.15)$$

Given that the concentration of H^+ ions can be calculated from the measured pH using:

$$[\text{H}^+] = \frac{-\log(\text{pH})}{\gamma_1} \quad (2.16)$$

a system of seven unknowns; $[\text{OH}^-]$, $[\text{CO}_2]$, $[\text{HCO}_3^-]$, $[\text{CO}_3^{2-}]$, $[\text{Ca}^{2+}]$, $[\text{CaHCO}_3^+]$ and $[\text{CaCO}_3^0]$ and seven equations; (2.6), (2.7), (2.8), (2.9), (2.10), (2.14) and (2.15) is obtained, which can be solved using the Maple™ Computer Algebra System.

The resulting functions for the seven unknowns in terms of total calcium and carbonate, ionic strength and acidity, e.g. $f([\text{OH}^-])(T_{Ca}, T_{Co}, I, [\text{H}^+])$, are used as input for the numerical step.

The solutions of the seven unknowns are presented in appendix A.

2.3 Numerical Solution

To find the T_{Ca} and T_{CO} from the measured EC and pH two additional balances are needed. The equations are presented below as root functions, meaning that they converge to zero for the correct values of T_{Ca} , T_{CO} , I and $[H^+]$.

$$f_1(T_{Ca}, T_{CO}, I, [H^+]) = EC - SC_{OH^-} - SC_{H^+} - SC_{HCO_3^-} - SC_{CO_3^{2-}} - SC_{Ca^{2+}} - SC_{Na^+} - SC_{Cl^-} - SC_{CaHCO_3^+} \quad (2.17)$$

$$f_2(T_{Ca}, T_{CO}, I, [H^+]) = [H^+] + [CaHCO_3^+] + 2 \cdot [Ca^{2+}] - [OH^-] - [HCO_3^-] - 2 \cdot [CO_3^{2-}] \quad (2.18)$$

Root equation 2.17 states that the measured conductivity (EC) has to be equal to the sum of the conductivity of all individual components in the solution.

Root equation 2.18 governs the electrical charge balance of the solution, which must always be zero.

2.3.1 Specific Conductivity

The conductivity, or specific conductance, is defined as the ability of an ionic solution to conduct electric charge and is the reciprocal of the resistance. It can be used as an indicator for the amount of ions available in the solution (Appelo, 2010).

The specific conductance of a solution can be calculated from the sum of a species concentration multiplied by its molar conductivity using:

$$SC = \sum \Lambda_m^0 \cdot m \quad (2.19)$$

Where:

SC	= Specific Conductance		[S/m]
Λ_m^0	= molar conductivity		[S/m/(mol/m ³)]
m	= concentration		[mol/m ³]

The molar conductivity of a species is governed by its diffusion coefficient and the concentration.

The relation between the diffusion coefficient and the molar conductivity is given by:

$$\Lambda_m^0 = \frac{z^2 F^2}{RT} D_w \quad (2.20)$$

Where:

Λ_m^0	= molar conductivity		[S/m/(mol/m ³)]
z	= charge number		[-]
F	= Faraday's constant		[Coulomb/mol]
R	= gas constant		[J/°K/mol]
T	= absolute temperature		[K]
D_w	= diffusion coefficient		[m ² /s]

The conductivity, however, does not linearly increase with the concentration. The influence of the concentration on the molar conductivity is given by Kohlrausch's law (Kohlrausch, 1870), which states that the molar conductivity decreases by the square root of the concentration, given by:

$$\Lambda_m = \Lambda_m^0 - K\sqrt{|z|m} \quad (2.21)$$

Where:

K	= Kohlrausch's Constant	[-]
z	= charge number	[-]
Λ_m	= Limiting molar conductivity	[S/m/(mol/m ³)]

Electrochemical Activity Coefficient

It is possible to approximate the value for Kohlrausch's constant K by introducing the electrochemical activity coefficient γ_{SC} (Appelo, 2010):

$$SC = \sum \Lambda_m^0 - K\sqrt{|z|m} = \sum \Lambda_m^0 \gamma_{SC} m \quad (2.22)$$

Which can, assuming γ_{SC} is close to 1, be rewritten to:

$$\gamma_{SC} \approx \exp\left(-\frac{K\sqrt{m}}{\Lambda_m^0} |z|^{1.5}\right) \quad (2.23)$$

Equation 2.23 can be compared with the limiting Debye-Hückel activity coefficient for low concentrations:

$$\gamma_{DH} = \exp(-\ln(10) \cdot 0.5\sqrt{m} \cdot |z|^2) \quad (2.24)$$

By multiplying the logarithm of γ_{DH} with a conversion factor f , the logarithm of γ_{SC} can be calculated:

$$f = \frac{K}{\Lambda_m^0 \cdot \ln(10) \cdot 0.5\sqrt{|z|}} \quad (2.25)$$

$$\gamma_{SC} = \gamma_{DH}^f \quad (2.26)$$

The empirical factors used are $f = 0.6/\sqrt{|z|}$ for ionic strength $I < 0.36 \cdot |z|$ and $f = \sqrt{I}/|z|$ for $I > 0.36 \cdot |z|$, which give a good approximation for the conductivity for solutions with a conductivity of 60mS/cm or lower. (Appelo, 2010).

The resulting expression for the specific conductance for solutions becomes:

$$SC = \sum \gamma_{DH}^f \cdot \frac{z^2 F^2}{RT} D_w \cdot m \quad (2.27)$$

The diffusion coefficients used for this model are presented in table 2.1.

Table 2.1: Overview of the diffusion coefficients used to calculate the electrical conductivity (Stumm and Morgan, 2012)

	Molecule	Charge number	Diffusion Coefficient
Cations	Ca ²⁺	2	0.79 · 10 ⁻⁹
	CaHCO ₃ ⁺	1	0.51 · 10 ⁻⁹
	Na ⁺	1	1.33 · 10 ⁻⁹
	H ⁺	1	9.31 · 10 ⁻⁹
Neutral	CaCO ₃ ⁰	0	0
Anions	OH ⁻	-1	5.27 · 10 ⁻⁹
	Cl ⁻	-1	2.03 · 10 ⁻⁹
	HCO ₃ ⁻	-1	1.18 · 10 ⁻⁹
	CO ₃ ²⁻	-2	0.96 · 10 ⁻⁹

2.3.2 Newton–Rhapson’s method

To find the roots of equations 2.17 and 2.18 Newton–Rhapson’s method was used. Newton–Rhapson’s method is a numerical method to solve nonlinear systems of equations which works by calculating the intersection points of linear n-dimensional tangent lines with the n-dimensional zero plane. From a given start position; the *initial guess*, the algorithm progressively walks closer to the solution of the system until a maximum number of steps is exceeded, or until the residuals of the root functions fall below the acceptable threshold (Vuik et al., 2007).

$$\begin{bmatrix} T_{Ca} \\ T_{CO} \end{bmatrix}_{i+1} = \begin{bmatrix} T_{Ca} \\ T_{CO} \end{bmatrix}_i - \begin{bmatrix} \frac{\delta f_1}{\delta T_{Ca}} & \frac{\delta f_1}{\delta T_{CO}} \\ \frac{\delta f_2}{\delta T_{Ca}} & \frac{\delta f_2}{\delta T_{CO}} \end{bmatrix}_i^{-1} \begin{bmatrix} f_1 \\ f_2 \end{bmatrix}_i \quad (2.28)$$

Although it is theoretically possible to analytically calculate the Jacobian matrix of the root functions, it is computationally far more efficient to make a two point guess of the derivative using forward Euler differentiation:

$$\frac{\delta f_n}{\delta x_n} \approx \frac{f_n(x_n + h) - f_n(x_n)}{h} \quad (2.29)$$

As initial guesses for T_{CO} and T_{Ca} a value of 1 mmol was used. For the ionic strength an initial guess of 10^{-2} was used, which was recalculated every step of the algorithm. The algorithm was repeated for 20 steps, with a numerical differentiation step-size h of 10^{-8} mol. The chosen initial conditions and stepsizes resulted in good convergence, with an average compound error of 10^{-13} [-].

The source code for the command line utility is included in appendix B and is written in the Swift 2.2 programming language (Apple, 2014) for a hundredfold increase in calculation speed when compared to Python and MATLAB™.

2.4 Model Validation

2.4.1 Method

To validate the model a batch reactor experiment was performed where 1.5 mmol of $\text{Ca}(\text{OH})_2$ was added to 500ml demineralized water containing 4 mM CaCl_2 and 8 mM NaHCO_3 . Nitrogen gas was used to form a closing layer on the surface of the water, preventing reactions with the surrounding air to take place.

Whilst continuously measuring the EC and pH during a period of 3 minutes every 15 seconds a 5 ml sample was taken from the reactor using a syringe. The sample was then immediately pressed through a $0.20\mu\text{m}$ screw-on filter to instantly stop the dissolution reaction. From the filtrate a 1 ml sample was taken and immediately diluted with 9 ml of deionized water to lower the Saturation Index (SI) of CaCO_3 and prevent further CaCO_3 precipitation from happening.

The samples were analyzed using two IC machines. To measure the calcium a Metrohm 883 Basic IC Plus was used using a Metrosep C 4-150/4.0 column. As eluent 0.3 mM nitric acid solution was used. The flow rate of the eluent was 0.9 ml/min and the sample size was 20 μL . A description of the procedure can be found in appendix C.

The carbonate was measured using a Metrohm 881 Compact IC Pro combined with a Y3-ICE9860 organic acids column heated to 50 degrees Celsius. As eluent 0.5 mM sulphuric acid solution was used. 50 mM LiCl solution was used as suppressor and the flow rate of the eluent was 0.7 ml/min. The sample size was 20 μL . A description of the procedure can be found in appendix D.

The conductivity of the output of the columns of both machines over time was measured and recorded. The area below the peaks corresponding to calcium and carbonate were measured and compared with peaks for a series of standard calcium and carbonate solutions.

2.4.2 Results

The results of the validation experiment are presented in figures 2.2 and 2.3. In figure 2.2 the measured values for pH and EC are presented. The calculated values from T_{Ca} and T_{CO} , as well as the values measured using the IC analyzer are presented in figure 2.3.

As can be seen in figure 2.3, the output of the presented model and the values measured by the IC machines closely correspond, especially from $t = 50\text{s}$ and onwards for calcium. The discrepancy between the measured and calculated total calcium in the first 50 seconds can likely be attributed to the failure of the pH sensor to adequately follow the rapid change in the solution acidity. In subsequent measurements (see the red line in figure 3.6 on page 27), with a newer and thus faster pH sensor, the initial hump in total calcium can be identified.

The calculated value of total carbonate gives a good prediction of the actual value of T_{CO} for the first 90 seconds of the experiment, but underestimates the T_{CO} for remainder of the experiment. This may have been caused by CaCO_3 precipitation on the conductivity sensor electrodes, resulting in a lower measured conductivity and thus a lower calculated T_{CO} .

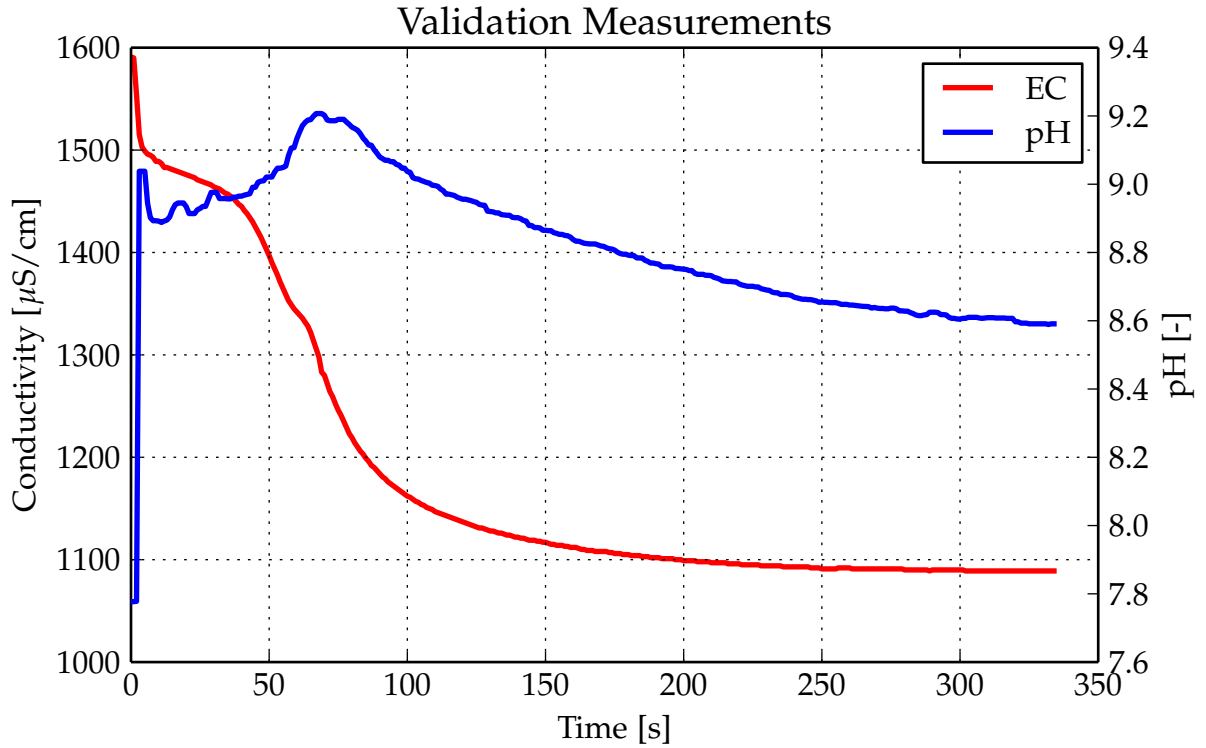


Figure 2.2: Online measured values of EC and pH during the validation experiment. The measured values for pH are lagging in the first fifty seconds of the experiment.

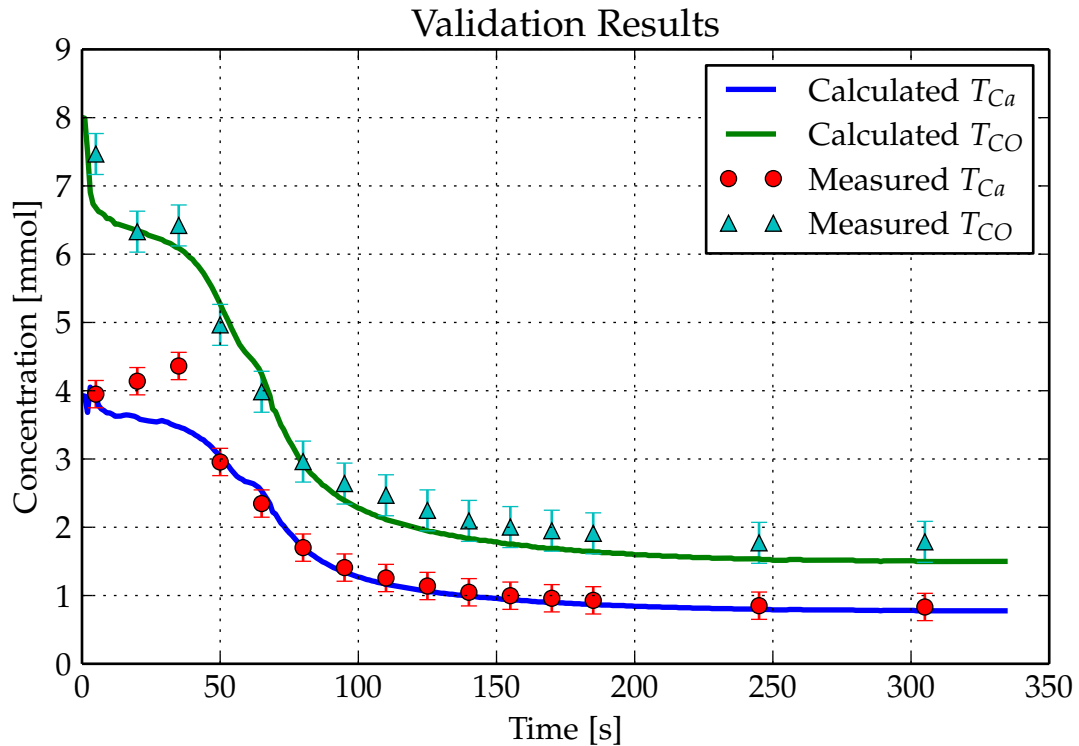


Figure 2.3: Output of the model compared with results from the ion-exchange chromatography analyzer.

Chapter 3

The Kinetics of Calcium Hydroxide Dissolution in Carbonate Containing Water

3.1 Introduction

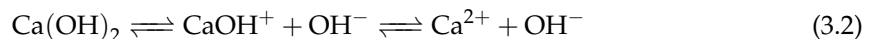
Calcium hydroxide, $\text{Ca}(\text{OH})_2$, is a fine white powder that is formed from the rapid reaction of calcium oxide, CaO , with water, a process called *slaking* (Ritchie and Bing-An, 1990).



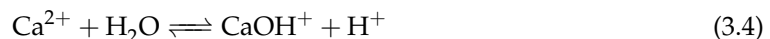
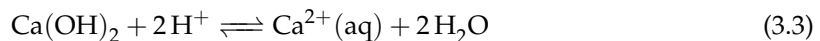
In water treatment processes calcium hydroxide is mainly used as a softening chemical (Van Eekeren and van Paassen, 1994), or to raise the pH of the water (Moel et al., 2006). Due to its low solubility $\text{Ca}(\text{OH})_2$ is often dosed as a suspension (*milk-of-lime*) rather than as a solution (*lime water*). Special suspensions of microscopically small lime particles, called *stable milk-of-lime*, have been developed to maximize reactivity and to reduce sedimentation problems in the storage tanks (Van Eekeren and van Paassen, 1994).

3.1.1 Dissolution in Pure Water

In pure water calcium hydroxide forms the following equilibrium:



Which can be reformulated to:



With $\log k_1 = 22.8$ and $\log k_2 = -12.78$ (Stumm and Morgan, 2012), which means that only 20.3 mmol of $\text{Ca}(\text{OH})_2$, about 1.5 gram, can dissolve in 1 kilogram of pure H_2O .

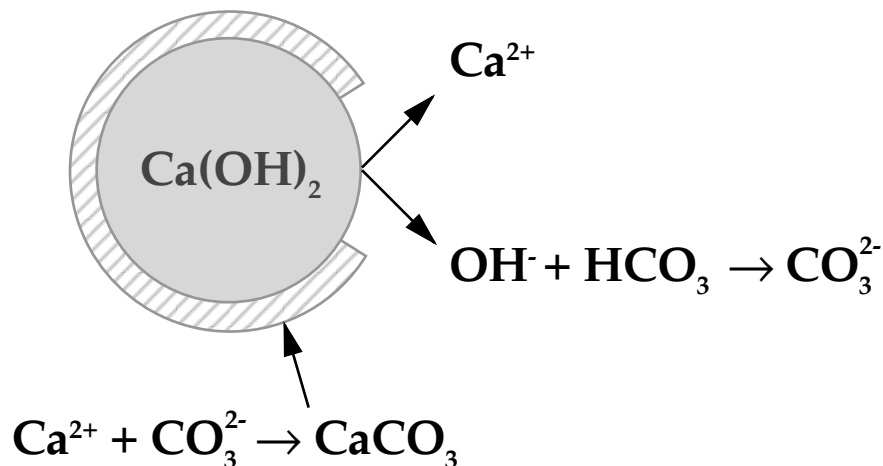


Figure 3.1: Schematic diagram of the Dissolve–Precipitate mechanism (Van Eekeren and van Paassen, 1994)

Kinetics of Dissolution in Pure Water

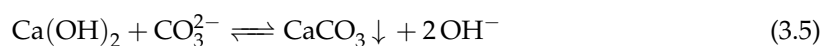
The dissolution rate of calcium hydroxide in pure water has been studied by several researchers (Giles et al., 1993; Johannsen and Rademacher, 1999; Van Eekeren and van Paassen, 1994).

Giles et al. used rotating disks of compressed lime partially submerged in water, and used continuous conductivity and intermittent Atomic Absorption Spectrophotometry (AAS) measurements to track the dissolution of $\text{Ca}(\text{OH})_2$ over time. By varying the disk rotation speed Giles et al. found that the rate of dissolution is diffusion limited at low mixing, and chemically limited at high mixing.

The dissolution of suspensions of lime particles was found to closely fit the *shrinking–sphere* model (Kamatani et al., 1980), which assumes that the particles are spheres with initial radius r_0 with a constant diffusion of Ca^{2+} and OH^- ions away from the $\text{Ca}(\text{OH})_2$ surface (Johannsen and Rademacher, 1999; Giles et al., 1993).

3.1.2 Dissolution in Carbonate Containing Water

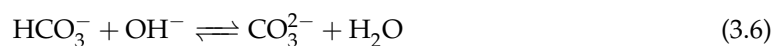
When added to carbonate containing water the Ca^{2+} and double OH^- ions dissociating from the $\text{Ca}(\text{OH})_2$ particles react with the (bi)carbonate in the water to form calcium carbonate:



Calcium carbonate has an extremely low solubility in water and therefore immediately starts to precipitate on the surface of the dissolving particle, an effect termed the *dissolve–precipitate* mechanism (Van Eekeren and van Paassen, 1994) (Figure 3.1).

A more accurate description, however, is the *dissolve–reprecipitate* mechanism as carbonate ions were found to not topochemically convert the $\text{Ca}(\text{OH})_2$ to CaCO_3 , but react with the Ca^{2+} and OH^- ions to form CaCO_3 which then precipitates on the $\text{Ca}(\text{OH})_2$ surface. This results in many small ‘islands’ of nucleated CaCO_3 to form on the $\text{Ca}(\text{OH})_2$ particle surface, which will

eventually coalesce to a covering layer of CaCO_3 (Galan et al., 2015).



If the solution into which the Ca(OH)_2 dissolves contains calcium ions in addition to bicarbonate (HCO_3^-) ions it is possible for up to twice as much CaCO_3 to form as Ca(OH)_2 was added, as a single molecule of Ca(OH)_2 can convert two molecules of bicarbonate to carbonate. This effect of effectively removing calcium from the water is termed *softening* and is the working principle behind Ca(OH)_2 —fed pellet softening reactors (Van Eekeren and van Paassen, 1994).

Kinetics of Dissolution in Carbonate Containing Water

The layer of calcium carbonate, partially blocking the surface of the dissolving calcium hydroxide, was found to result in a reduced reaction rate (Van Eekeren and van Paassen, 1994) for Ca(OH)_2 particles, or, for large crystals, prevents complete dissolution from happening (Galan et al., 2015).

Most of the research, however, has been done towards the kinetics of the dissolution of calcium oxide in carbonate containing water, a process somewhat similar to that of Ca(OH)_2 . In a rotating disk study, similar to the one performed by Giles et al. (1993), Xu et al. (1998) found that the concentration of carbonate ions in the water had great influence on the decrease in dissolution rate of the CaO disk. A relatively low concentration of carbonate resulted in a patchy layer of CaCO_3 crystals forming on the disk surface, only mildly slowing the dissolution rate. Moderate concentrations of carbonate resulted in a much denser and uniform layer of CaCO_3 , greatly reducing the dissolution rate. High concentrations of carbonate, however, resulted in a more chaotic formation of CaCO_3 crystals resulting in the dissolution kinetics increasing again.

For powdered CaO Xu et al. (1998) tracked the dissolution by measuring the temperature rise in the solution and found again that the dissolution rate was greatly reduced by the carbonate in the water. Interpretation of the results however proved to be difficult due to the dissolution of CaO being an exothermic and the formation of CaCO_3 being an endothermic reaction.

Dissolve-Precipitate-Break mechanism

The results of one experiment are of great note. In this experiment Xu et al. (1998) found that “For the solution containing 0.01 M sodium carbonate, the initial slaking was fast, but after about 30 s the rate of change of temperature fell off, only to speed up again after about 2 min of reaction and finally reaching an equilibrium temperature after about 4 min of reaction.”

A possible explanation for this phenomenon can be found in the research by Song and Kim (1990) towards the dissolution of pre-carbonated CaO particles. They found that, after an induction period, the protective layer would crack and break due to the stresses created by the slowly dissolving particle inside, and the formation of Ca(OH)_2 islands between the CaCO_3 layer, allowing the dissolution to continue at a rapid rate.

Dissolution Mechanism of Calcium Hydroxide in Carbonate Containing Water

Knowledge on the dissolution mechanism of $\text{Ca}(\text{OH})_2$ in carbonate containing water however, is still highly limited. Thus, in this study, a method is presented to interpret the changes in electrical conductivity and acidity of the solution during the dissolution reaction using the soft-sensor presented in chapter 2.

3.2 Materials and Methods

3.2.1 Batch Experiments

To determine the dissolution rate of the calcium hydroxide and the formation rate of calcium carbonate batch dissolution experiments were conducted in a glass reactor. Different dosages of milk-of-lime were added to 500 mL solutions of demineralized water containing CaCl_2 and NaHCO_3 stirred using a teflon magnetic stirring bar at 600rpm. The reactor was continuously flushed with nitrogen gas to form a gas blanket on the water surface, preventing interactions with the carbon dioxide in the outside air to take place.

The milk-of-lime was made by adding 9.25 gram of >98% pure calcium hydroxide powder with a particle size of 1–10 μm to 250 mL of water in a glass erlenmeyer to form a 0.5 M suspension. The milk-of-lime was continuously stirred using a teflon magnetic stirring bar and separated from the outside air using a N_2 -gas blanket.

After the dosing of the lime with a calibrated digital pipette the changes in the conductivity and acidity of the solution were measured for a duration of 300 seconds, after which the experiment was terminated. The measured values were stored in a comma-separated-values (CSV) file, which in turn was used as input for a command-line application for further processing.

The measured EC and pH were converted to 25 °C reference values by the sensors. Therefore no correction for the temperature was necessary.

After each experiment the reactor, stirring bar, and sensors were rinsed with a weak acid to remove CaCO_3 depositions formed during the experiment.

Solution Used

The solution used in all experiments was a 4 mM CaCl_2 , 8 mM NaHCO_3 solution. This solution has an Saturation Index (SI) of 1.27 for calcite and gives an approximation of the concentrate of a NF treatment plant treating calcium-rich groundwater with a recovery of sixty to seventy percent.

Due to the high supersaturation of calcite the calcium chloride and sodium bicarbonate were each added separately to the reactor, shortly before the start of each experiment, to prevent premature precipitation of CaCO_3 from occurring. First the sodium bicarbonate was added, and after the acidity of the solution stabilized, the calcium chloride was added.

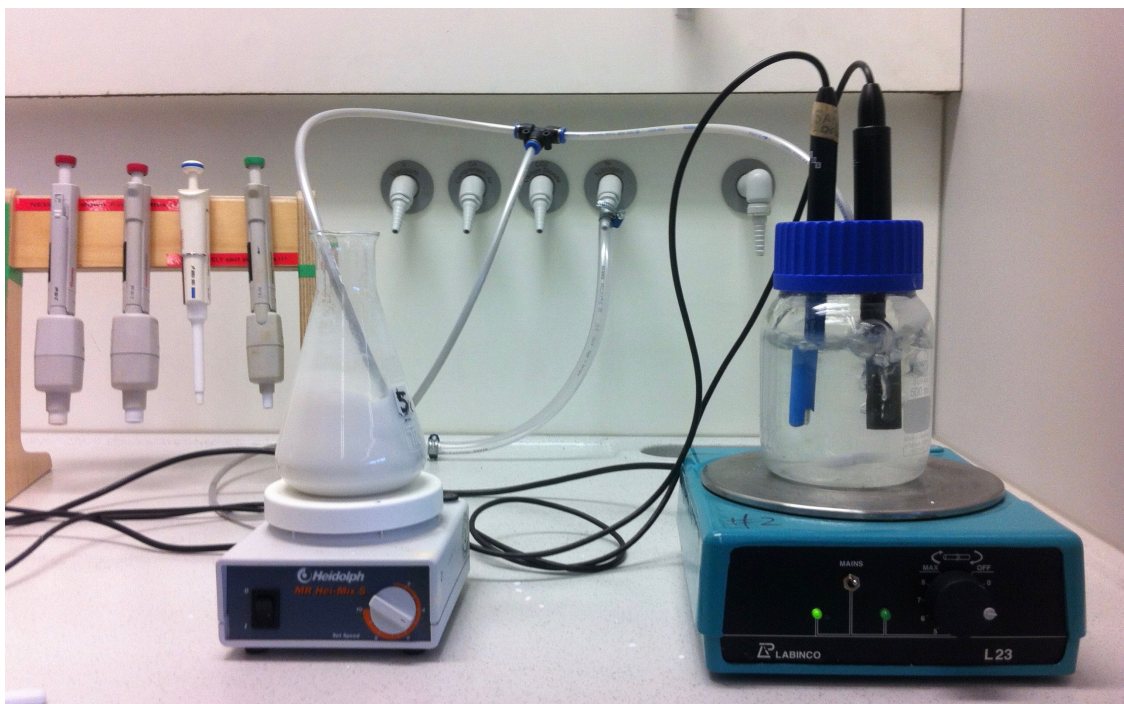


Figure 3.2: Photo of the experimental setup used to determine the dissolution kinetics of slaked lime in carbonate containing water.

Data Conversion and Interpretation

The soft-sensor for calculating total calcium T_{Ca} and total carbonate T_{CO} from the measured EC and pH presented in chapter 2 was used to determine the amount of lime dissolved and the amount of CaCO_3 precipitated.

With the total amount of calcium and carbonate in the solution, as well as their initial concentrations, known, it is possible to calculate the amount of lime dissolved and CaCO_3 precipitated using the following two mass-balances:

$$\text{CaCO}_3 \text{ Precipitated} = \text{Initial Carbonate} - \text{Carbonate In Solution} \quad (3.8)$$

$$\text{Lime Dissolved} = \text{Calcium In Solution} - \text{Initial Calcium} + \text{CaCO}_3 \text{ Precipitated} \quad (3.9)$$

3.3 Results and Discussion

3.3.1 Effect of Lime Dissolution and CaCO₃ Formation on the Conductivity and Acidity

In order to determine the effect of the amount of Ca(OH)₂ dissolved and CaCO₃ formed on the electrical conductivity and pH of the solution the numerical part of the model presented in chapter 2 was modified. Instead of the T_{Ca} and T_{CO} now only the $[H^+]$ remains unknown. It is therefore sufficient to only evaluate root function 2.18 on charge.

$$f_2(I, [H^+]) = [H^+] + [CaHCO_3^+] + 2 \cdot [Ca^{2+}] - [OH^-] - [HCO_3^-] - 2 \cdot [CO_3^{2-}]$$

A meshed grid of values for the T_{Ca} and T_{CO} in a 4mM CaCl₂ and 8mM NaHCO₃ solution was entered as model input. The results of the calculation, in terms of formed CaCO₃ and dissolved Ca(OH)₂ are presented in figure 3.3.

As can be seen in the surface plot for the conductivity, by following the green line, the dissolution of lime, in this solution, initially results in an increase in total molecules in the solution, yet causes a *decrease* in electrical conductivity. This counter-intuitive effect can be explained by the rapid formation of still dissolved CaCO₃⁰ molecules from HCO₃⁻ ions converted to CO₃²⁻ by the added OH⁻ ions. After more than four mmol of Ca(OH)₂ has dissolved, however, the HCO₃⁻ ions are almost completely removed from the solution, causing the conductivity to rise again.

The formation of CaCO₃ results, when little to no lime has dissolved, in a rapid decrease in conductivity as the concentration of dissolved CaCO₃⁰ is initially very low. When more lime has dissolved the concentration of the non-conducting CaCO₃⁰ molecules is much higher. Therefore, removal from the solution at that moment results in a more gradual decrease of conductivity.

On the surface plot for the acidity two points of inflection can be identified, corresponding with the carbonic-acid-bicarbonate-carbonate equilibrium points. Precipitation of CaCO₃ shifts the balance to the left, thus reducing the pH. Dissolution of Ca(OH)₂ increases the basicity of the solution by the addition of OH⁻ ions, shifting the balance to the right and leading to an increase in pH.

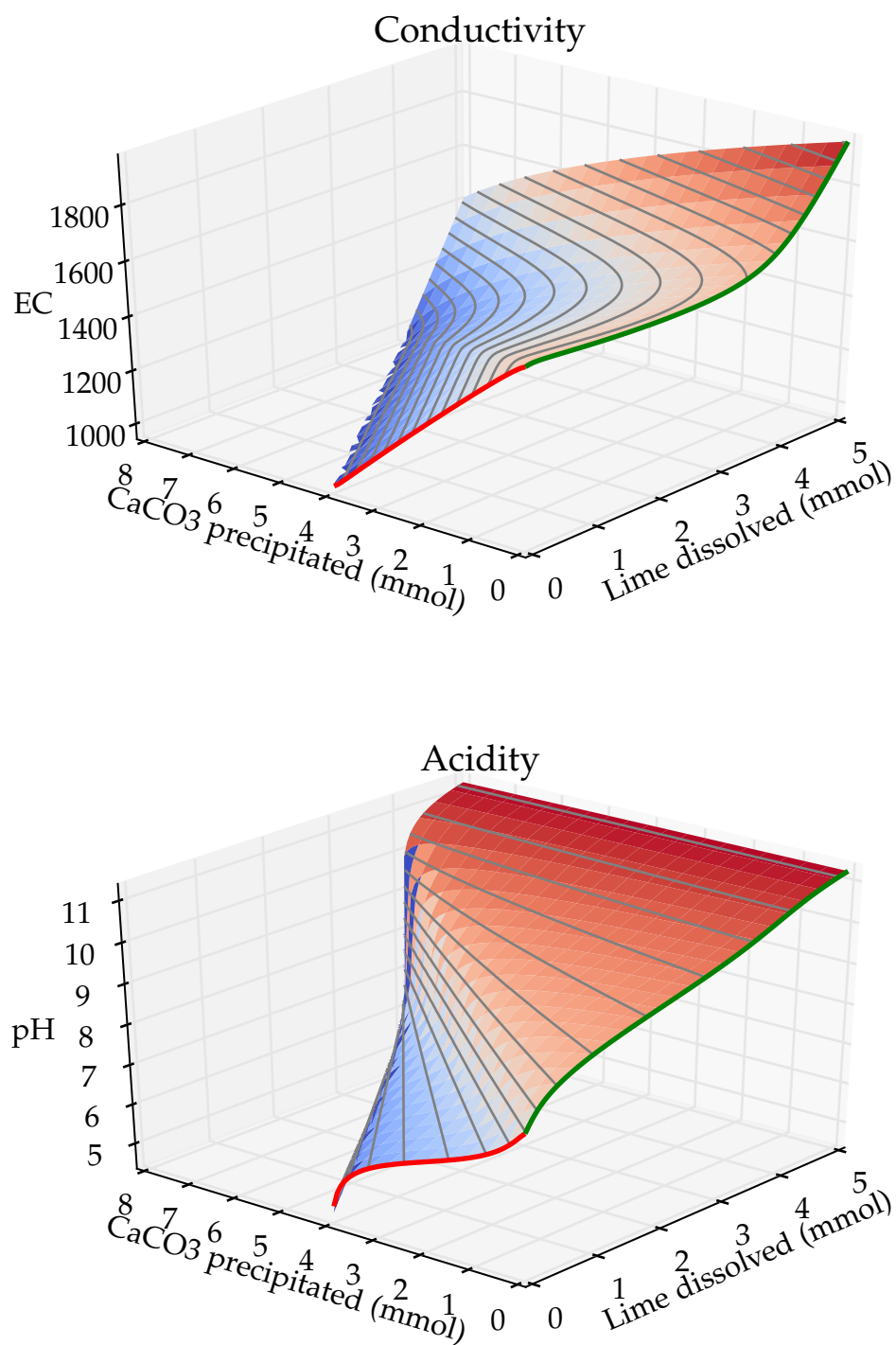


Figure 3.3: Surface plots of the influence of the amount of lime dissolved and CaCO_3 precipitated on the electrical conductivity (top) and on the acidity (bottom) of a 4mM CaCl_2 , 8mM NaHCO_3 solution, calculated using the model presented in this chapter. The red lines follow the x-axis (CaCO_3 formed), the green lines follow the y-axis (Ca(OH)_2 dissolved)

3.3.2 Dissolution Kinetics of Calcium Hydroxide in Carbonate Containing Water

To determine the dissolution kinetics of $\text{Ca}(\text{OH})_2$ in carbonate containing water twelve batch reactor experiments were done, with $\text{Ca}(\text{OH})_2$ dosages of 1 to 6 mmol *per liter* in pure water and in the 4mM CaCl_2 , 8mM NaHCO_3 solution.

The results of the experiments, processed by the model described in chapter 2, are presented in figures 3.4 to 3.7.

As can be seen in figure 3.4, the dissolution in pure water (dashed lines), occurs rapidly and follows the *shrinking-sphere* model as was previously determined by Giles et al. (1993) and Johannsen and Rademacher (1999).

When added to the carbonate containing solution, however, in addition to the expected reduction of dissolution rate due to the dissolve-precipitate effect, a secondary effect can be seen to take place for dosages of 2 mmol $\text{Ca}(\text{OH})_2$ per liter and higher. As was previously seen by Xu et al. (1998) for the dissolution of calcium oxide, the reactions initially are fast, but reduce rate after around 30 seconds, only to speed up again later.

Dissolve-(Re)precipitate-Break-Collapse Effect

A proposed explanation for this phenomenon can be found by looking at the change in solution composition (figures 3.6 , 3.7 and 3.9) over time.

The following four phases can be identified:

1. Dissolution
2. Precipitation
3. Stress Induction
4. Particle Collapse

The time of occurrence of the four phases for the dissolution reaction of 4 mmol $\text{Ca}(\text{OH})_2$ is annotated in figure 3.8. A schematization of the proposed dissolution mechanism is presented in figure 3.10.

Dissolution

During the first ten seconds of the reaction around half of the calcium hydroxide is dissolved, resulting in a peak in total calcium concentration. Simultaneously, calcium carbonate crystals begin to immediately form in the solution, resulting in a sharp decline in the total carbonate concentration.

Re-Precipitation

At ($T=10$), after the initial rapid dissolution, the formed calcium carbonate crystals start to precipitate on the surface of the $\text{Ca}(\text{OH})_2$ particles, greatly reducing their dissolution rate. The coverage of the calcium carbonate layer on the surface of the particles can be seen to differ with the amount of $\text{Ca}(\text{OH})_2$ dosed.

3. The Kinetics of Calcium Hydroxide Dissolution in Carbonate Containing Water

For the relatively low dosages of 1 and 2 mmol per liter the reduction of dissolution rate is limited as most of the Ca(OH)_2 is already dissolved before enough calcium carbonate is formed to precipitate on the surface of the particles. The highest reduction in dissolution rate takes place for the dissolution of 4 mmol Ca(OH)_2 per liter, for which the reaction almost halts for a period of 60 seconds.

For higher dosages of 5 and 6 mmol Ca(OH)_2 per liter the reaction speeds up again. This can be attributed to the either higher total surface area of the particles, or to the faster and more chaotic formation of CaCO_3 , resulting in a less densely covering layer of CaCO_3 to form,

Stress Induction

As the protective layer of CaCO_3 is not completely sealing the Ca(OH)_2 particles the dissolution continues, albeit at a much lower rate. The particles keep shrinking, whilst more CaCO_3 forms on the outside, introducing shear stresses on the both the particle and its protective layer.

Particle Collapse

After an induction period of thirty to fifty seconds, depending on the coverage of the protective layer, the formation rate of CaCO_3 suddenly increases. This causes the stress on the particle and the protective layer to further increase until they collapse and break apart. The fragments of Ca(OH)_2 rapidly dissolve, causing a sudden and large increase in the calcium concentration. Afterwards, due to the high amount of calcium now in the solution, more CaCO_3 rapidly forms until an equilibrium is formed or all of the carbonate is removed from the solution.

Softening Reaction

As was expected from the softening theory presented in section 3.1.2, the final amount of CaCO_3 formed is limited by the amount of hydroxide ions added to the solution, with 1 mmol of Ca(OH)_2 resulting in the formation of 2 mmol of CaCO_3 , 2 mmol of Ca(OH)_2 in 4 mmol CaCO_3 , etc.

The model however overestimates the amount of CaCO_3 precipitated for dosages five and six mmol per liter of Ca(OH)_2 , resulting in a negative calculated carbonate concentration at the end of the experiment. As the total Ca(OH)_2 dissolved is predicted correctly the most likely explanation for the discrepancy is the deposition of CaCO_3 on the conductivity sensor's electrodes.

The resulting decrease in measured conductivity results in a higher calculated amount of CaCO_3 formed, whilst the calculated amount of Ca(OH)_2 dissolved remains almost the same, as can be seen in figure 3.3.

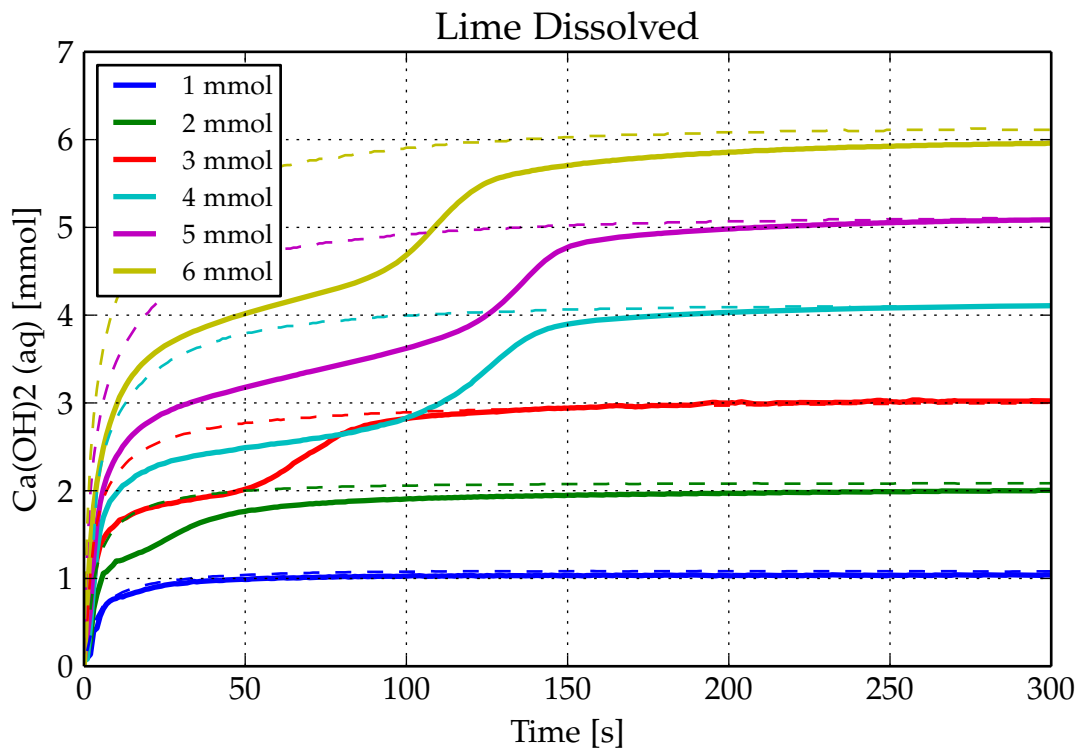


Figure 3.4: Calculated amount of Ca(OH)_2 dissolved over time. The dashed lines indicate the dissolution of Ca(OH)_2 in pure water.

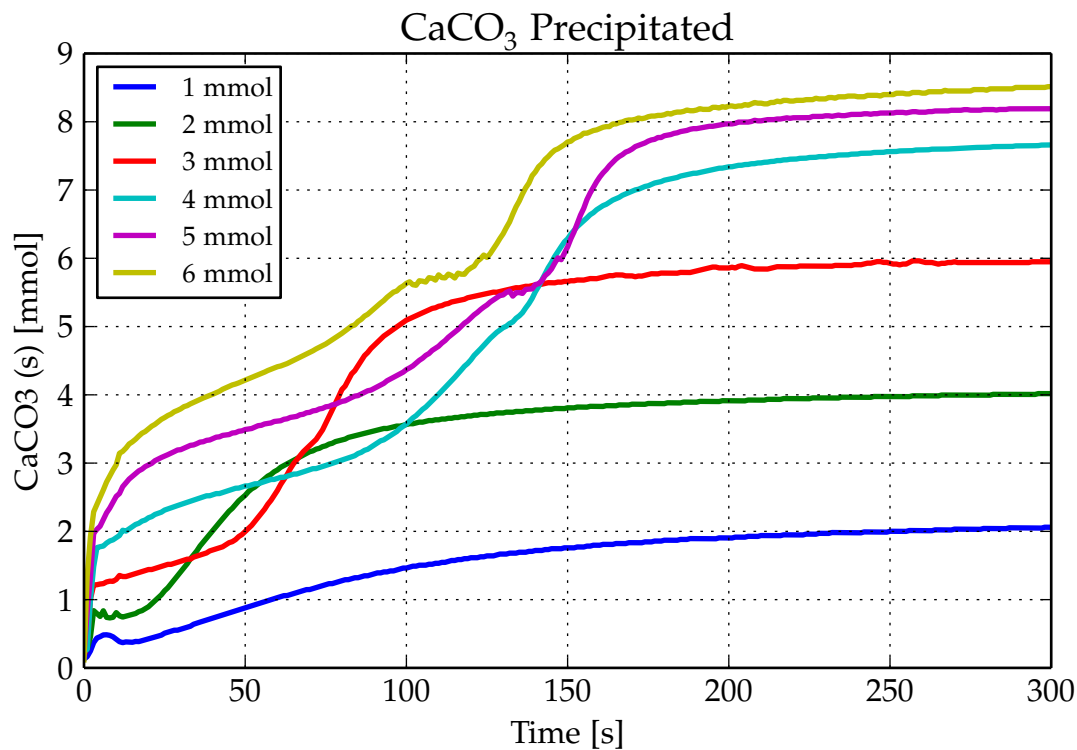


Figure 3.5: Amount of CaCO_3 precipitated over time

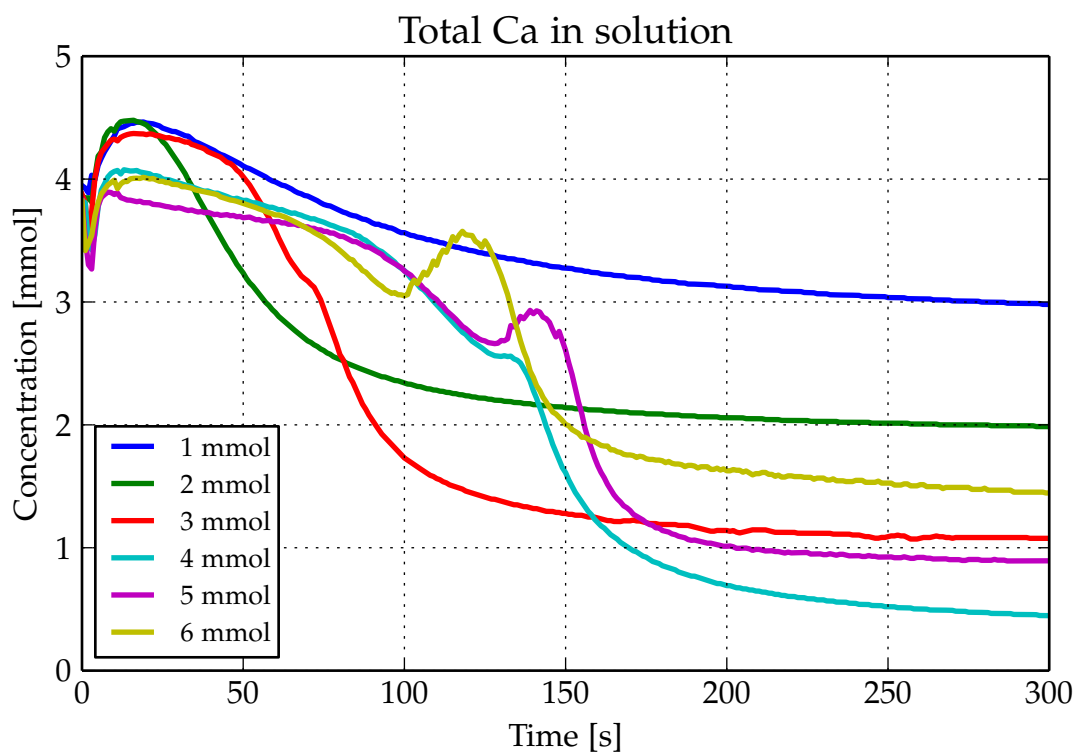


Figure 3.6: Calculated concentration of total calcium in the solution over time

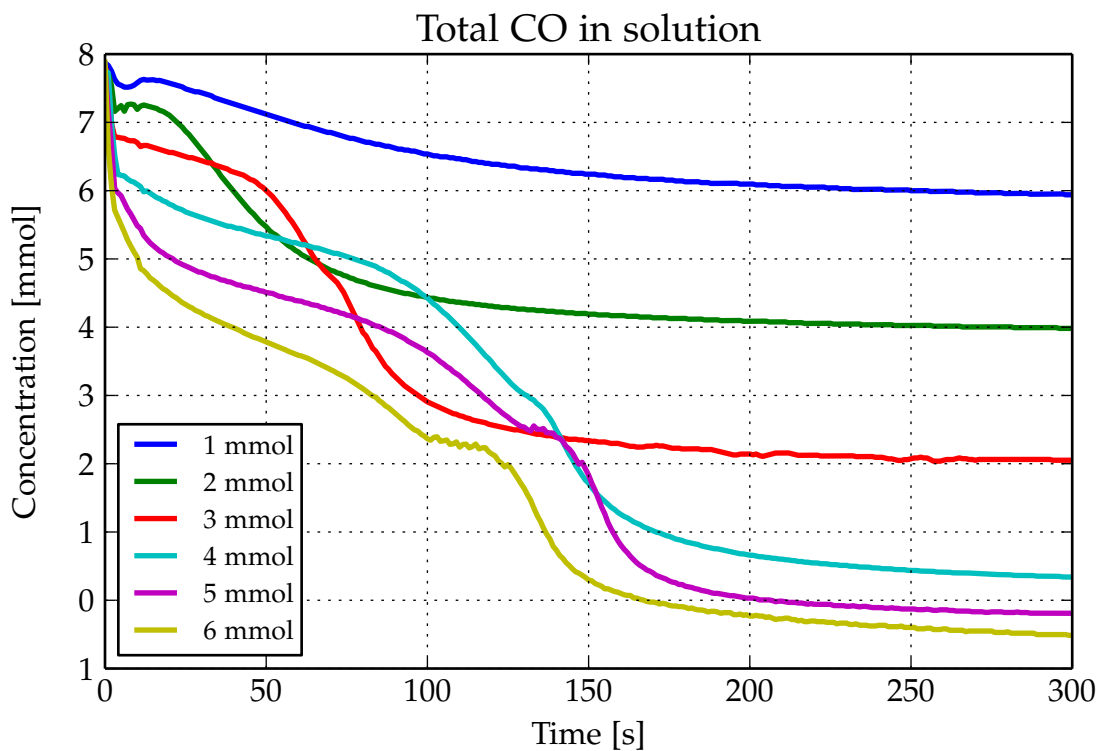


Figure 3.7: Calculated concentration of total carbonate in the solution over time

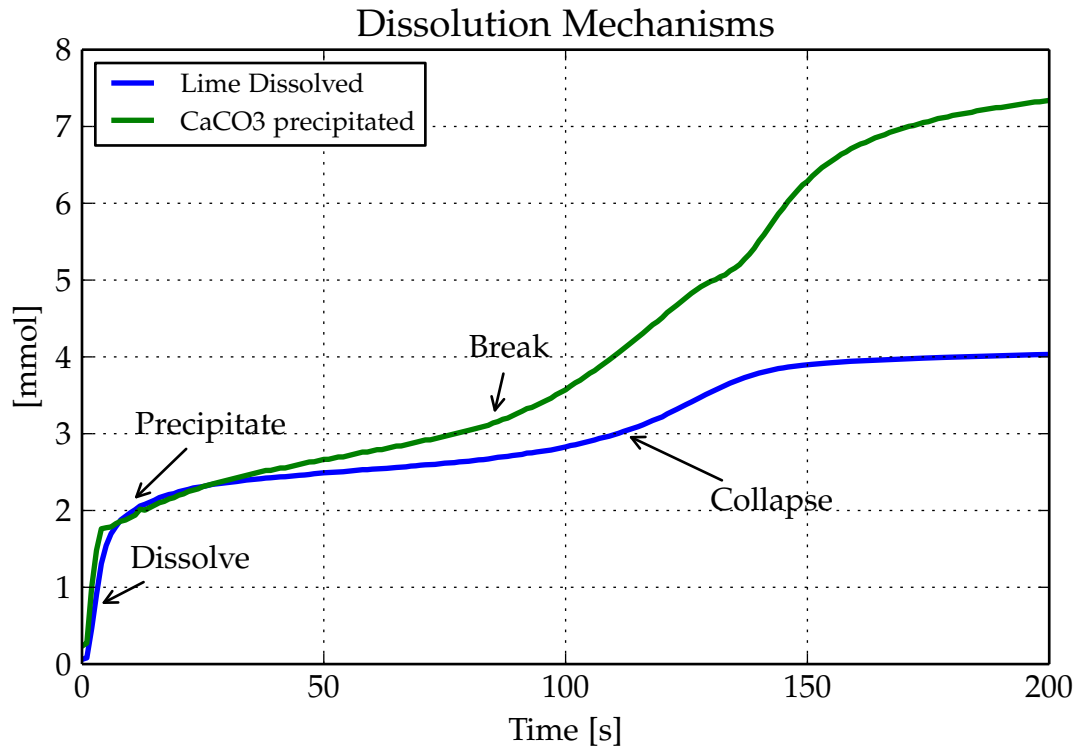


Figure 3.8: Time of occurrence for the four dissolution phases of the dissolution of 4 mmol Ca(OH)₂ in a 4mM CaCl₂, 8mM NaHCO₃ solution

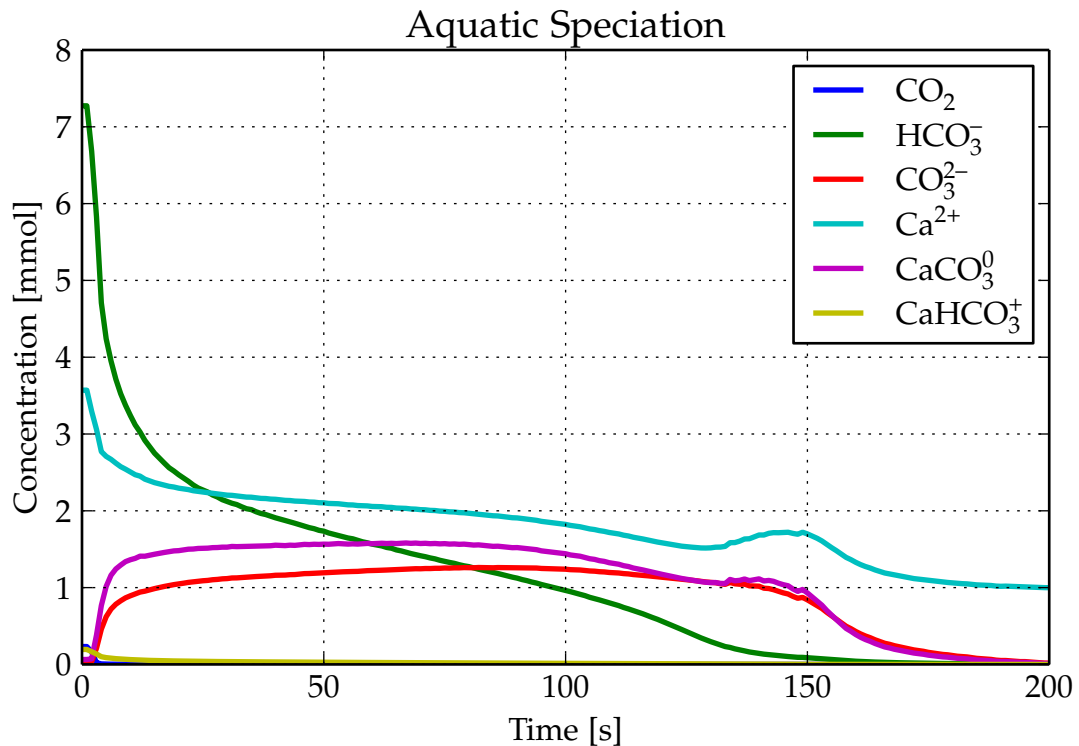
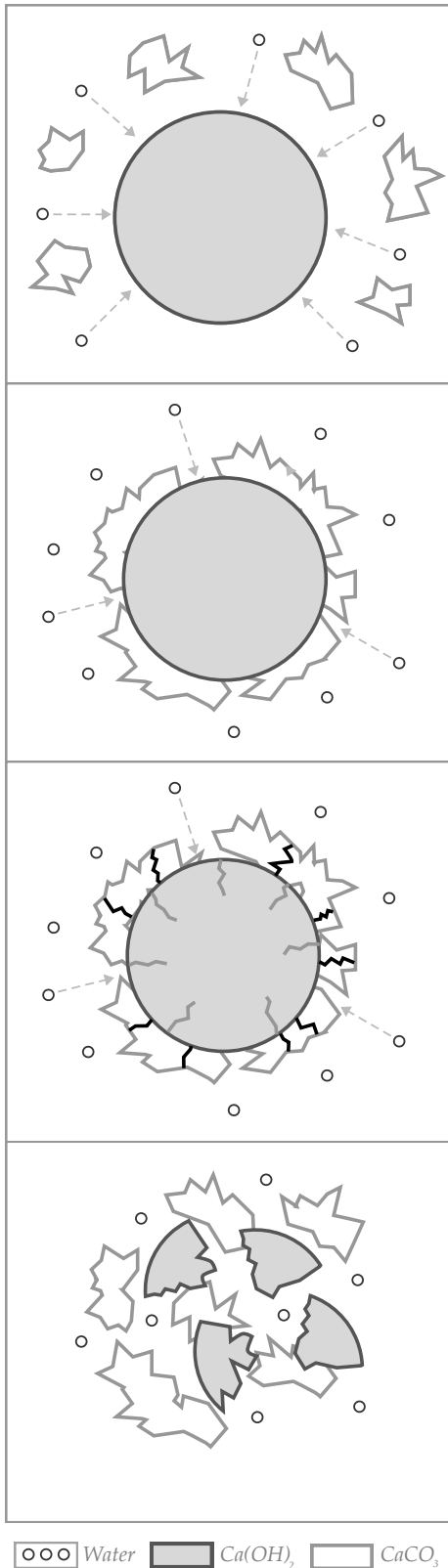


Figure 3.9: Calculated Aquatic speciation distribution over time for the dissolution of 5 mmol Ca(OH)₂ in a 4mM CaCl₂, 8mM NaHCO₃ solution



1. Dissolution

The Ca(OH)_2 particle has just been added to the solution, and reacts with water to form Ca^{2+} and OH^- ions, which in turn react with the HCO_3^- in the reaction to form CaCO_3 crystals.

2. Precipitation

The CaCO_3 crystals settle on the surface of the Ca(OH)_2 particle, forming a protective layer which slows down the dissolution reaction.

3. Stress Induction

Because the protective layer of CaCO_3 does not completely seal the Ca(OH)_2 particle's surface, the particle keeps shrinking, while simultaneously more CaCO_3 forms. This introduces shear stress on the Ca(OH)_2 particle and the protective layer.

4. Particle Collapse

When the stress becomes too high the particle and its protective layer break, allowing the dissolution reaction to continue.

Figure 3.10: Schematization of the dissolve-precipitate-break-collapse mechanism.

Chapter 4

Calcium Hydroxide as Precipitative Antiscalant for Nanofiltration

4.1 Introduction

With the dissolve–precipitate effect of calcium hydroxide confirmed it is now possible to test whether it can be used as antiscalant for calcium carbonate scaling.

To test the principle flat-sheet NF membranes were used instead of a conventional, spiral wound ones. Not only did this allow for rapid replacement of the membrane for each experiment, visual inspection during the experiments and experiments without a feed spacer were, with this type of membrane, possible. In addition, the smaller cross–section of the flat–sheet membrane requires a much smaller flow to attain the same crossflow velocity when compared to spiral wound modules.

The pilot plant was simulated to be treating the concentrate of a NF treatment plant treating calcium–rich groundwater with a recovery of 60–70 percent. The lime dosing is thus not used for the whole filtration process, only for the final element in the chain. The simulated location is depicted in figure 4.1.

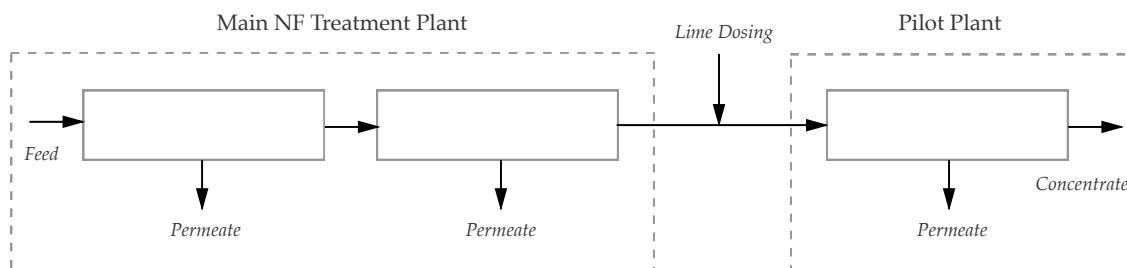


Figure 4.1: Simulated location of the pilot treatment plant, further treating the concentrate of a larger NF treatment plant.

4.2 Materials and Methods

In total four (successful) experiments have been performed to determine whether slaked lime particles can be applied as a precipitative antiscalant for NF membrane filtration. To simplify the experiment, and therefore provide a proof-of-concept, only scaling by CaCO_3 was simulated. Two experiments were done with an added 28 mil feed spacer and two experiments were done without spacer.

4.2.1 Experimental Setup

The experiments were performed using a custom-designed and built flat-sheet membrane filtration pilot installation (figure 4.2 and 4.3).

From a feed tank demineralized water, kept at a constant 25°C by a temperature control bath connected to a heat exchanger, was pumped through a flat sheet membrane container by a rotary-vane positive-displacement pump. The level in the feed tank was kept at a constant level by means of a flapper valve connected to the centralized demi-water installation of the Waterlab. The permeate and concentrate were contaminated by the experiments and therefore had to be discarded.

Three injection points for the addition of calcium chloride (CaCl_2), sodium bicarbonate (NaHCO_3) and milk-of-lime (Ca(OH)_2) were added. The NaHCO_3 had to be added before the pump and the CaCl_2 after, in order to prevent premature scaling from disrupting the functioning of the pumpheads vanes. NaHCO_3 was dosed from a airtight bag-in-a-box using a peristaltic pump to prevent interactions with the surrounding air. The CaCl_2 and Ca(OH)_2 had to be added under pressure and were therefore dosed using two diaphragm pumps. A nitrogen gas blanket was used to separate the Ca(OH)_2 from the atmosphere.

Using four valves in a cross arrangement the direction of the flow could be switched between forward and reverse. In the concentrate stream an injection point for compressed air was added to allow for air-enhanced backwashing.

The pressure in the system was regulated using a solenoid control valve and was measured at three places; in the feed water, halfway the membrane container and in the concentrate water. In addition to measuring the pressure the volumetric flow rate of the feed and permeate was measured, as well as the conductivity and temperature of the feed, concentrate and permeate.

The pressure vessel contained an 0.18 m² AlfaLaval NF flat sheet membrane with a MgSO_4 rejection of >98% (see appendix E for the full specifications).

Control System and Data Acquisition

To operate the system a fully automated control system was developed based on an Arduino Mega microprocessor which continuously monitored the eleven connected sensors and the status of the demiwater tank and dosing systems.

To operate the system at a constant recovery Proportional-Integral-Derivative (PID) controllers were used. One PID controller directly regulated the rotational speed of the electric motor driv-

ing the pump by comparing the readout from the feed flow impeller with the chosen setpoint for feed flow.

Directly controlling the solenoid control valve position based on the measured permeate flow proved to be unstable due to the relatively low sampling frequency of the permeate flow sensor. Therefore a dualstage PID control system was introduced. The first controller regulated the pressure setpoint based on the measured permeate flow, and the second controller regulated the control valve position based on measured pressure and the given setpoint for pressure. The high sampling frequency of the pressure sensor resulted in a much smoother control of the valve position. In addition, problems with *integral windup*; the tendency of the PID controller to accumulate a significant error during transition to a setpoint causing excess overshooting, could be avoided.

Measured data was sent at an interval of 5 seconds from the Arduino Mega to a connected Raspberry PI singleboard computer, which relayed the data to an InfluxDB timeseries database instance running on a “cloud” server for analysis and sampling.

4.2.2 Experimental Procedure

Before the start of each experiment the flat-sheet NF membrane in the pressure vessel was replaced with a new one and run-in with demiwaterr for a duration of at least six hours.

During the experiments a constant feed flow of 50 liter per hour and constant recovery of 10 percent was used, resulting in a cross-flow velocity of 0.09 m s^{-1} and a flux of $27.8 \text{ L m}^{-2} \text{ h}^{-1}$. The cross-flow velocity was limited by the capacity of the demiwaterr-installation in the CiTG laboratory and could therefore not be increased further.

Measurements

During the experiments the increase in MRC was measured and used as an indicator for scaling:

$$K = \frac{TMP}{\mu J} \quad (4.1)$$

Where:

K	= Membrane Resistance Coefficient		$[\text{m}^{-1}]$
J	= Volumetric Flux		$[\text{m}/\text{s}]$
TMP	= Trans Membrane Pressure		$[\text{N}/\text{m}^2]$
μ	= Dynamic Viscosity of Water		$[\text{Ns}/\text{m}^2]$

The TMP is defined as net pressure difference over the membrane:

$$TMP = \Delta P - \Delta \pi \quad (4.2)$$

Where:

ΔP	= Hydraulic Pressure Difference		$[\text{N}/\text{m}^2]$
$\Delta \pi$	= Osmotic Pressure Difference		$[\text{N}/\text{m}^2]$

For these experiments the ΔP was defined as the pressure measured in the middle of the membrane vessel as the permeate pressure was atmospheric.

The influence of the osmotic pressure difference was, for each separate experiment, considered to be a constant factor for the duration of the experiment. It was therefore not taken into account when considering the increase of MRC as indicator for scaling.

Conductivity measurements in the feed and concentrate stream proved to be too unreliable to use due to CaCO_3 deposits forming on the sensor electrodes, resulting in either underestimated values, or in extreme cases, no conductivity measurement at all.

Chemical Dosing

As feed water the same solution used for the batch experiments was used, simulating calcium-rich groundwater at 60–70 percent recovery. The solution consisted of 4 mmol CaCl_2 and 8 mmol NaHCO_3 per liter.

A slaked lime dosage of 2 mmol per liter was chosen based on the results of the batch experiments. As can be seen from figure 3.5 on page 26 this dosage results in a high formation rate of CaCO_3 from 10 seconds onwards, at which time the slaked lime just enters the pressure vessel.

The dissolve-precipitate-break-collapse mechanism for higher dosages was deemed unwanted for this particular experiment, as it would result in the bulk of the softening reaction to take place *outside* the pressure vessel. For filtration systems with longer retention times, however, the extended dissolution reaction may prove useful as the $\text{Ca}(\text{OH})_2$ particles stay 'active' for a longer duration.

Reverse-Flow Washing procedure

To prevent $\text{Ca}(\text{OH})_2$ and CaCO_3 particles from accumulating in the system and on the membrane surface an air-enhanced washing sequence was used. The necessity of this process can clearly be seen on the photos of the membrane surface taken by the USB-microscope before and after backwashing (figure 4.4).

The following 50 second wash programme was used after comparing the results of several alternatives:

T = 0s Turn off the main and dosing pumps and open the control valve to relieve pressure

T = 3s Change the flow direction to reverse and run the main pump at 100% capacity

T = 10s Inject compressed air at 6 bar for 1.5 seconds

T = 20s Inject compressed air at 6 bar for 1.5 seconds

T = 30s Change the flow direction to forward

T = 40s Return to previous PID-controlled setpoint

T = 50s Turn on chemical dosing pumps

The wash programme was automatically started every hour, or when the pressure difference over the membrane container exceeded 1 bar.

4. Calcium Hydroxide as Precipitative Antiscalant for Nanofiltration

The automatic backwash routine was performed also when no lime particles were dosed to rule out its influence on the scaling process.

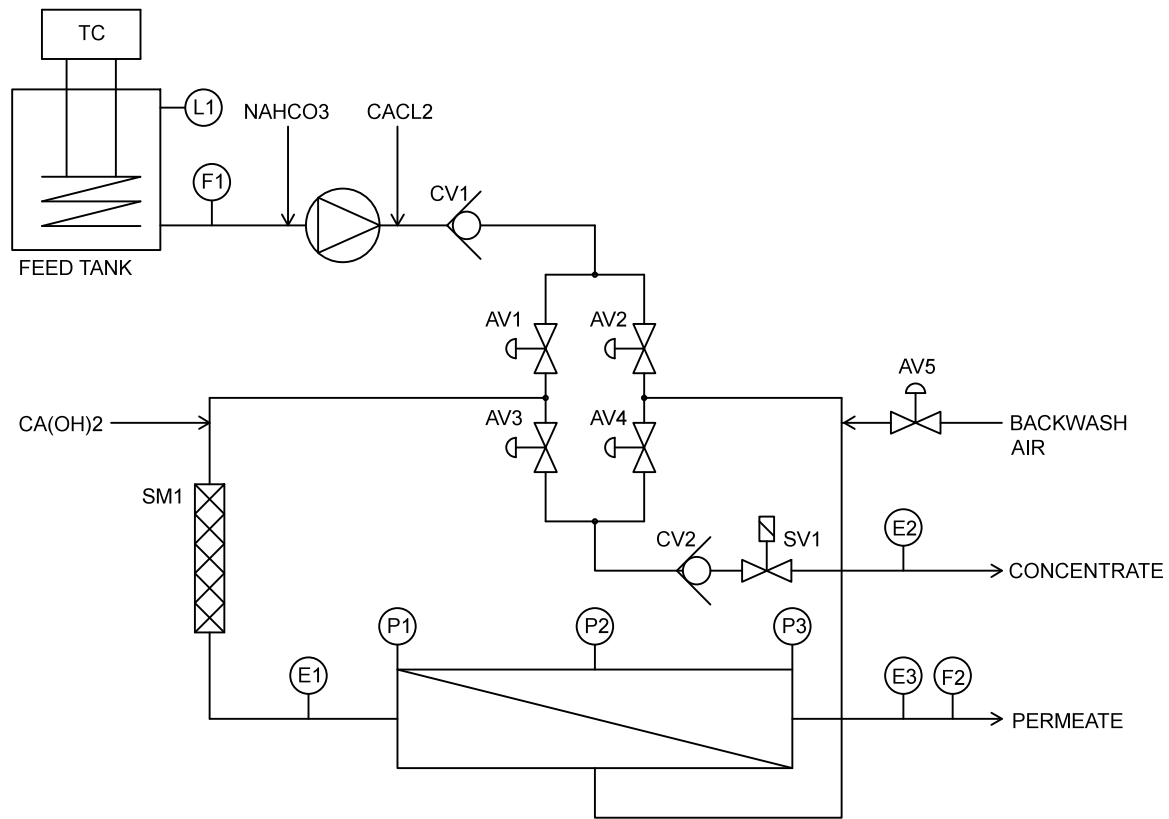
Duration of Experiments

The experiments were run until either the feed pressure exceeded 8 bar, or when the interval between two backwashes fell below 15 minutes. An emergency shutdown procedure, instantly opening the control valve and halting the main pump, was activated when the pressure anywhere inside the system exceeded 9 bar to prevent damage to the valves and fittings.

Optical Inspection

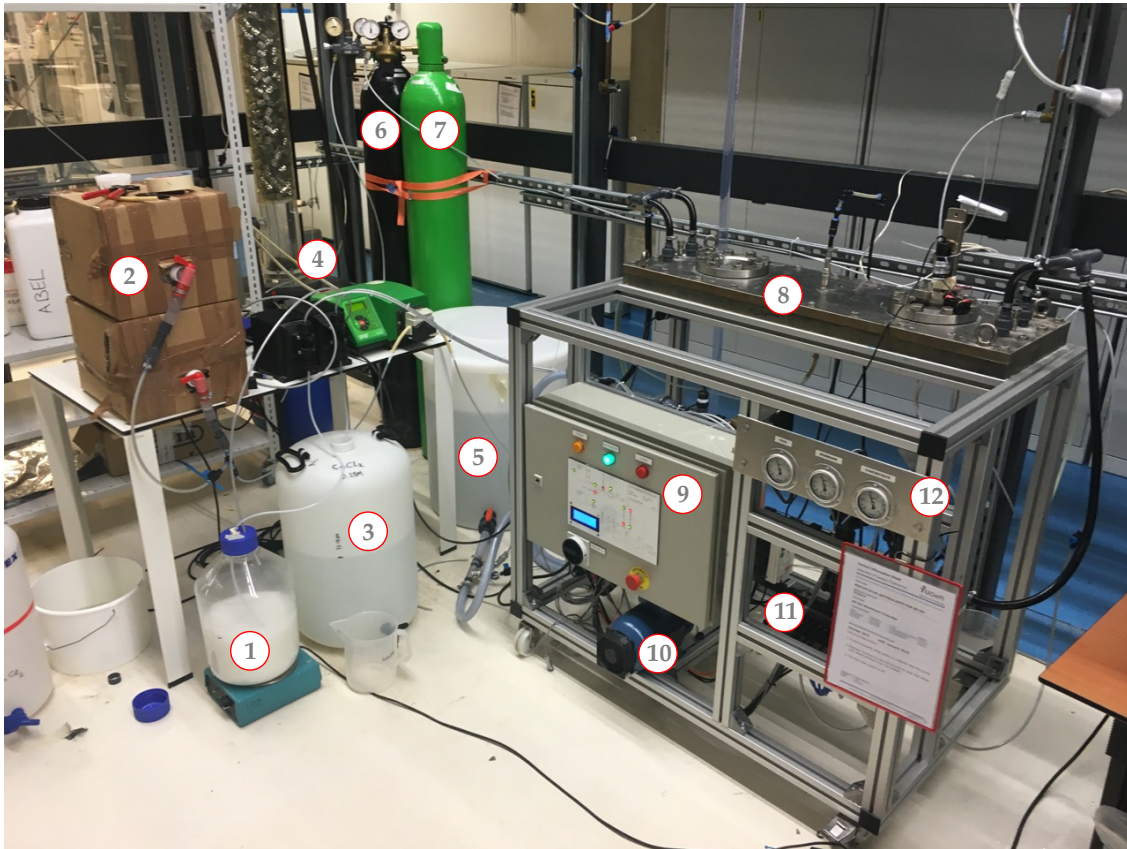
During the experiments a photo of the condition of the membrane surface was taken every five minutes through the inspection glass on the membrane vessel using a USB-microscope. To highlight the white CaCO_3 particles on the white membrane UV light with a wavelength of 380nm was used.

After completion of the experiments the flat sheet membrane was removed from the pressure container and placed under an optical microscope to inspect the amount and type of scaling on the membrane surface.



TC	Temperature Control Bath	P1	Feed Pressure
L1	Level Sensor	P2	Membrane Pressure
F1	Feed Flow Impeller	P3	Concentrate Pressure
CV1,2	Check Valves	SV1	Solenoid Control Valve
AV2,3	Forward Direction Valves	AV5	Backwash Air Valve
AV1,4	Reverse Direction Valves	E2	Concentrate Conductivity
SM1	Static Mixer	E3	Permeate Conductivity
E1	Feed Conductivity	F2	Permeate Flow Impeller

Figure 4.2: Schematic overview of the experimental setup. During normal operation the water valves AV2 and AV3 are closed, and water moves through the system in a counter-clockwise manner. During backwash operation valves AV1 and AV4 are closed, reversing the direction of the flow.



- | | |
|---------------------------------------|----------------------------|
| 1. $\text{Ca}(\text{OH})_2$ Container | 7. Compressed Air Cylinder |
| 2. NaHCO_3 Container | 8. Pressure Vessel |
| 3. CaCl_2 Container | 9. Control Electronics |
| 4. Injection Pumps | 10. Main Pump |
| 5. Demiwater Tank | 11. VFD and Air-Valves |
| 6. N_2 - Gas Cylinder | 12. Pressure Gauges |

Figure 4.3: Photo of the experimental setup in operation

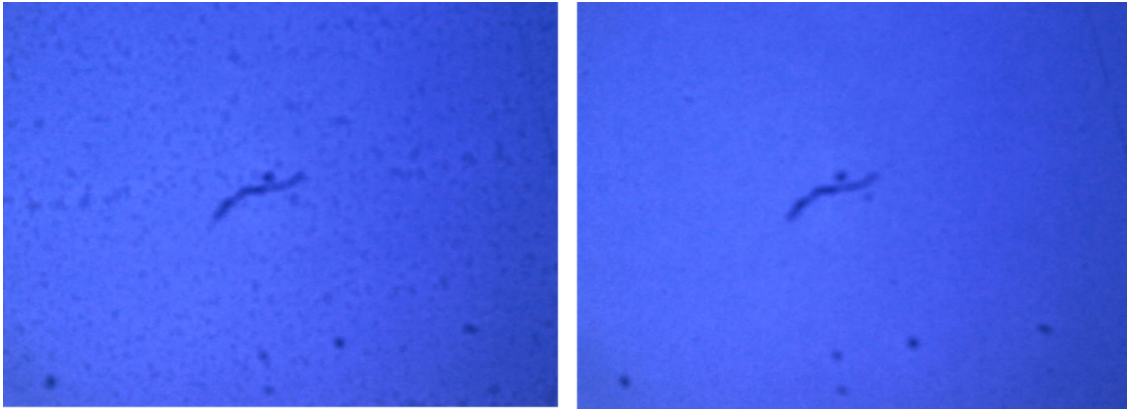


Figure 4.4: Photo of the membrane surface before (left) and after (right) backwashing. To illuminate the CaCO_3 particles UV light with a wavelength of 380nm was used. The large obstacle in the center of the photo is a visual defect caused by damage of the lens, not a particle on the membrane surface

Table 4.1: Overview of the four experiments performed

#	Description	Runtime	Halt condition
1	28–mil spacer, no lime	18h	Control System Failure
2	28–mil spacer, 2 mmol lime	6h	Backwash Frequency <15 min
3	No spacer, no lime	4.5h	Pressure > 8 bar
4	No spacer, 2 mmol lime	23h	Backwash Frequency <15 min

4.3 Results and Discussion

4.3.1 Pilot–Plant Experiments

The results of the four experiments performed are presented in figures 4.6 and 4.7

Without Lime Dosing

Without the dosing of lime a rapid increase in membrane resistance coefficient could be observed. The fastest rate of scaling took place when no spacer is installed. This can be explained by the higher concentration polarisation occurring due to the lack of turbulence caused by the feed spacer. The higher concentration polarisation caused by the absent spacer also results in a higher initial MRC.

Inspection with an optical microscope (figure 4.8) of the membrane surface confirms the presence of an blocking layer of CaCO_3 crystals after completion of the experiment.

Experiment 3, without feed spacer, was aborted after a mere four and a half hours due to the feed pressure exceeding 8 bar. Experiment 1, with a 28–mil feed spacer, was prematurely stopped after a control system failure caused by an overflowing integer value, but nonetheless gives a good insight in the scaling rate occurring.

With Lime Dosing

The addition of $\text{Ca}(\text{OH})_2$ had an immediate effect on the concentration polarisation, which was lowered due to the precipitation of CaCO_3 and the formation of still dissolved CaCO_3^0 ion-pairs without charge, resulting in an initially lower TMP and thus lower MRC.

$\text{Ca}(\text{OH})_2$ dosing in combination with a 28 mil spacer proved to be troublesome, as the particles did not transfer through the membrane vessel as wanted, but got trapped in the dead zones around the spacer. The air-enhanced backwash programme proved incapable of effectively removing the particles from the membrane vessel.

The accumulation of CaCO_3 particles on the membrane surface and around the spacer, clearly visible on figure 4.5, not only resulted in a gradual increase of MRC, but in a growing pressure loss between the feed and the concentrate side of the pressure vessel. This continuously triggered the automatic backwashing programme, until the interval fell below 15 minutes and the experiment was halted.

Without the 28-mil feed spacer the increase in MRC was non-existent for the first ten hours of the experiment, indicating that the added $\text{Ca}(\text{OH})_2$ particles help prevent CaCO_3 scaling on the membrane surface from taking place.

After the initial ten hours the MRC slowly started to increase. After fifteen hours of continuous operation the MRC started to increase at an accelerated rate. At the same time the automated backwash frequency started increasing, until at $T=23\text{h}$ the minimum interval of 15 minutes was reached and the experiment was halted.

Inspection with an optical microscope (figure 4.8) of the membrane surface indicates the occurrence of *bulk*-crystallization, instead of surface-crystallization. It is unclear, however, whether the deposits of loosely adherent CaCO_3 on the membrane surface were formed over the duration of the experiment, or are a result of the failing backwash procedure during the last hours of the experiment.

4.3.2 Particulate Fouling inside the System

An explanation for the increase in MRC and backwash interval during experiment 4 was found by inspecting the control system output. Instead of accumulating inside the pressure vessel, as was the case during experiment three, (part of) the CaCO_3 and $\text{Ca}(\text{OH})_2$ particles deposited inside the solenoid control valve. The resulting reduction of the valve opening's cross-section caused the control system to compensate by further opening the valve, as can be seen in figure 4.9, to maintain the same pressure. Initially the backwash cycle, identified by the hourly spikes in the output, manages to reverse the fouling, but after an extended period the fouling becomes permanent.

Although the fouling of the valve has little effect on the standard operation, as the pressure inside the system remains the same, it does have a large influence on the effectiveness of the backwash programme. The reduction of the valve orifice's cross-section drastically lowers the K_{vs} , defined as the amount of flow through the fully opened valve at a pressure difference of 1 bar.

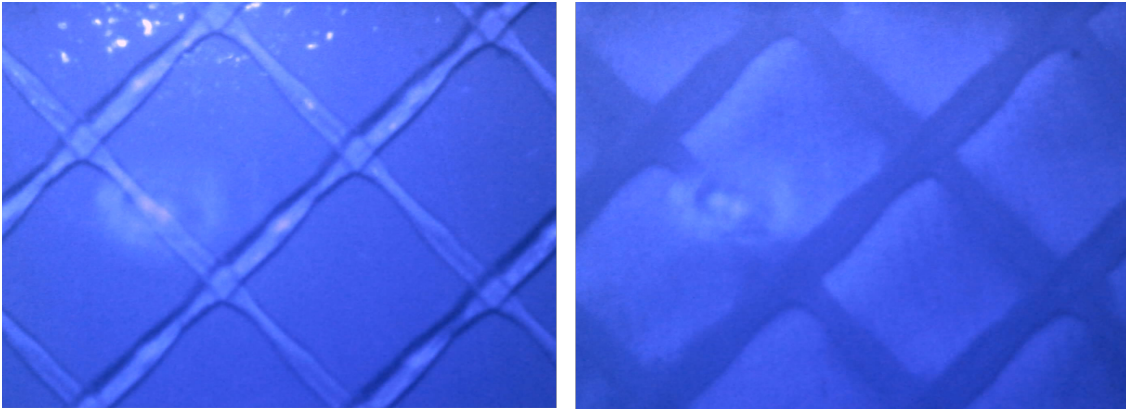


Figure 4.5: Photo of the membrane surface before (left) and after (right) completion of experiment 3. To illuminate the CaCO_3 particles UV light with a wavelength of 380nm was used.

The lower K_{vs} not only resulted in a lower backwash velocity, but, more importantly, caused the water pressure during backwashing to rise. This in turn reduced the effectiveness of the air-wash cycle and, when the backwashing pressure eventually rose above that of the compressed air system, caused the air-wash cycle to no longer take place at all.

Upon further inspection after dismantling part of the system, large amounts of CaCO_3 deposits were found in all the components upstream of the pressure vessel, further contributing to the decrease in hydraulic performance.

The inability of the backwash procedure to adequately remove the CaCO_3 particles trapped inside the pressure vessel could be observed after opening the vessel (figure 4.10). The accumulation was further worsened by the hydraulic design of the vessel, having only two small entry and exit ports.

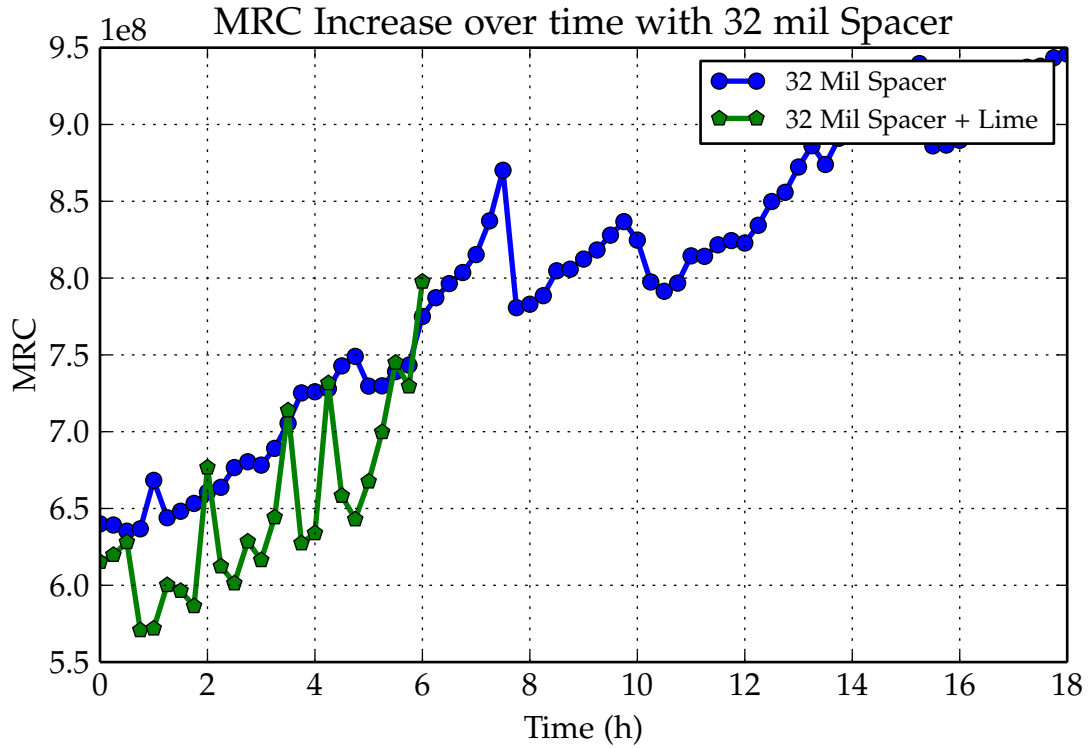


Figure 4.6: Increase of the Membrane Resistance Coefficient (MRC) over time with a 28-mil spacer

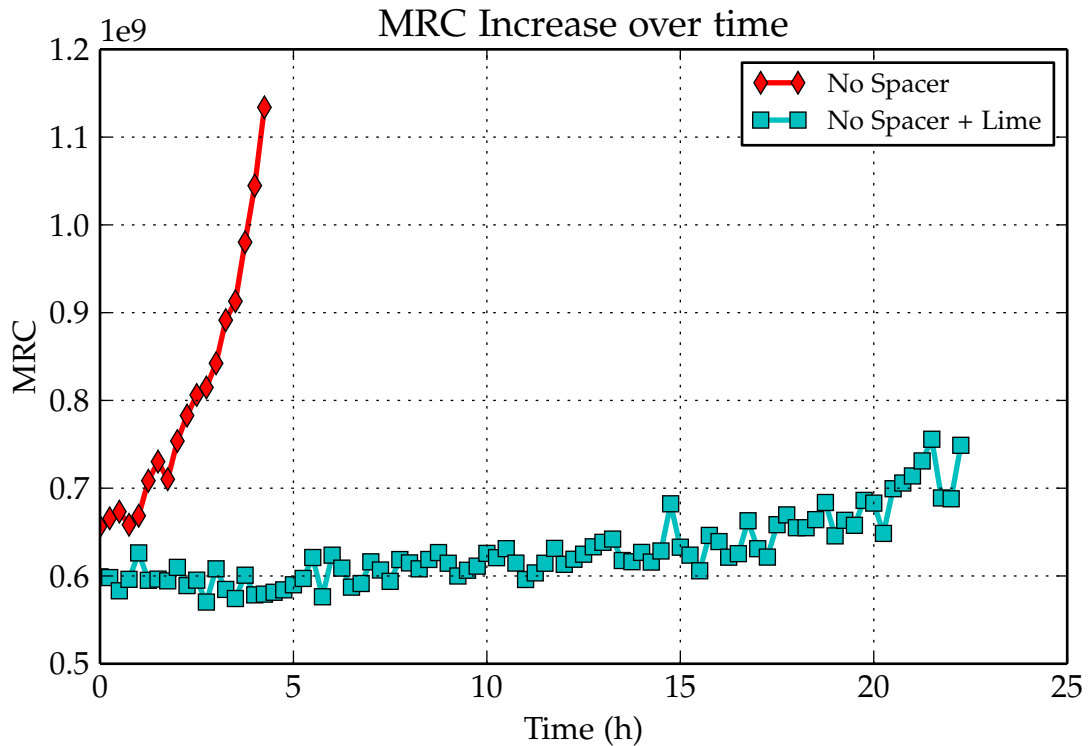


Figure 4.7: Increase of the Membrane Resistance Coefficient (MRC) over time when no spacer is used

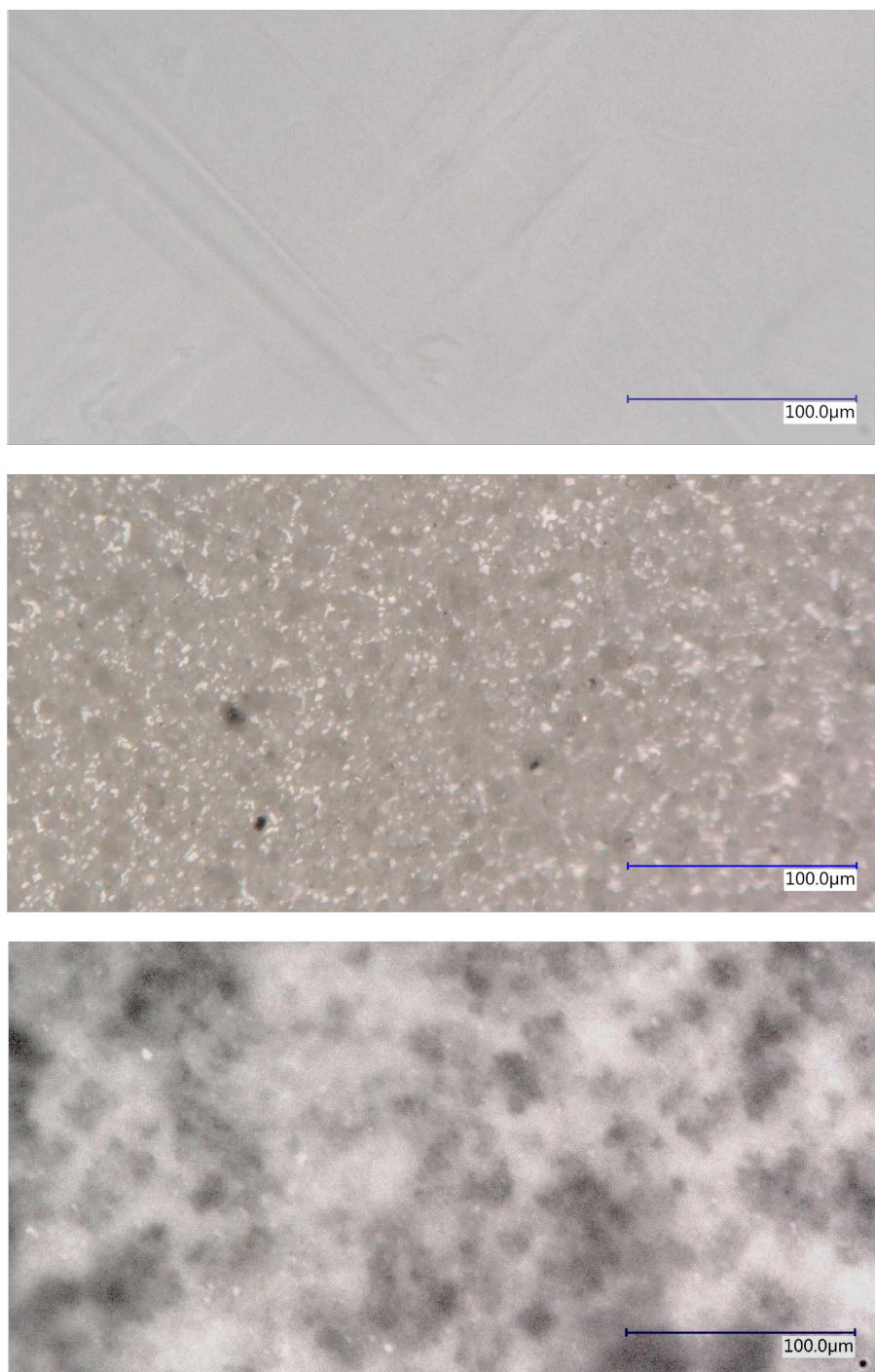


Figure 4.8: Microscope image of the clean membrane surface (top), after experiment 3 (middle) and experiment 4 (bottom). In the middle image crystal growth on the surface, corresponding with *surface*-crystallization, can clearly be identified. In the bottom picture the dominant scaling mechanism seems to be *Bulk*-crystallization, evidenced by the large deposits formed on the surface.

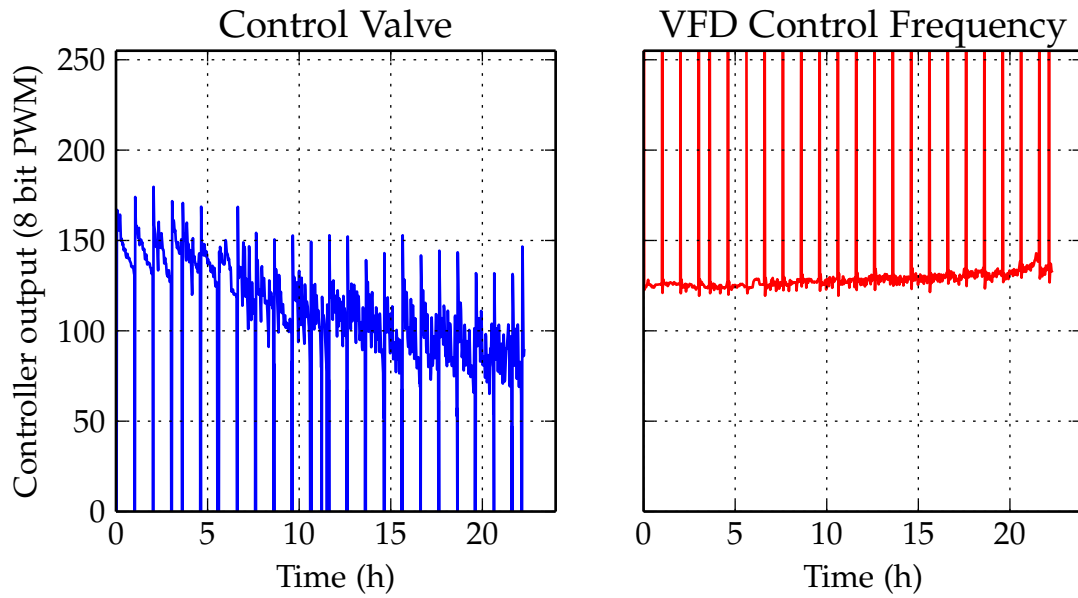


Figure 4.9: PID Controller output for the position of the control valve (left) and the variable frequency drive (VFD) output (right) during experiment 4



Figure 4.10: Accumulation of CaCO₃ deposits near the inlets of the pressure vessel after conclusion of experiment 4

Chapter 5

Summary and Conclusions

The four research questions presented in chapter 1 will be answered in the sections below.

5.1 Soft-Sensor for Total Calcium and Carbonate

1. *How can the total concentration of calcium and carbonate in a solution be calculated from the EC and pH?*

In chapter 2 a soft-sensor able to convert Electrical Conductivity (EC) and pH to total calcium T_{Ca} and total carbonate T_{CO} , was presented.

The sensor, based on chemical thermodynamics and mass-action balances, consisted of two components, an analytical and a numerical one. The analytical component was used to express all the relevant aquatic species occurring in terms of total calcium and total carbonate. The numerical part of the soft-sensor iteratively calculated the T_{Ca} and T_{CO} from the measured EC and pH using Newton-Raphsons method.

Although some simplifications and assumptions were made, the sensor was able to accurately predict the solution composition, as was confirmed by a validation experiment comparing the output of the model with that of the measured total calcium and carbonate.

The soft-sensor is thus a valuable tool, allowing for continuous measurement of the solution composition. This allows for a better insight into the reactions occurring. In addition, the model takes away the need for intermittent sampling, which not only costs a lot of time and is labour intensive, but may also influence the reactions occurring.

5.2 Dissolution of Calcium Hydroxide in Carbonate Containing Water

2. *What is the dissolve-precipitate mechanism of slaked lime, how much $CaCO_3$ can be formed on a particle, how can the process be influenced and what are the kinetics involved?*

The batch experiments performed and described in chapter 3, confirm the occurrence of a CaCO_3 layer forming on the Ca(OH)_2 particle surface, hindering dissolution as was previously found by Van Eekeren and van Paassen (1994) and Xu et al. (1998).

The extent of the blocking effect of the CaCO_3 layer was found to be dependent on the amount of Ca(OH)_2 added, with a dosage of 4 mmol per liter resulting in the highest coverage. For lower dosages the Ca(OH)_2 particles seem to dissolve before enough CaCO_3 has a chance to precipitate on the surface. For higher dosages the greater total surface area of Ca(OH)_2 seems to result in a less coalescent layer of CaCO_3 .

The amount of CaCO_3 precipitated follows the softening theory, being double that of the amount of Ca(OH)_2 dissolved. It is uncertain, however, how much of the CaCO_3 precipitates on the Ca(OH)_2 particles, and how much bulk crystallization has taken place.

In addition to the dissolve–precipitate mechanism a secondary effect takes place for high dosages of Ca(OH)_2 , with the dissolution rate increasing again after an extended period of time. This effect has been identified in previous studies by Xu et al. (1998) but no satisfactory explanation was available.

A possible explanation for the phenomenon, formulated with the aid of the previously introduced soft–sensor, is that the blocking layer of CaCO_3 is unstable and breaks after an extended period. This allows the dissolution reaction to continue at normal rate.

5.3 Calcium Hydroxide as Precipitative Antiscalant

3. *How do the Ca(OH)_2 particles behave inside a spaced NF membrane, do they get lodged between the spacers and if so, can they easily be removed by flushing with air?*
4. *Is it possible to prevent CaCO_3 scaling on the membrane surface by adding Ca(OH)_2 particles to the feed water to act as combined seed surface and softening chemical?*

The pilot plant and experimental procedure introduced in chapter 4 proved capable of simulating CaCO_3 scaling inside membrane filtration installations, with the fastest scaling occurring when no spacer is installed to reduce the concentration polarization. The occurrence of surface crystallization was confirmed by inspection with an optical microscope.

When dosing Ca(OH)_2 the 28–mil spacer proved to be of significant hindrance for the Ca(OH)_2 and CaCO_3 particles, which tended to get stuck between the spacer elements and could not be flushed out during the cleaning cycle.

Without a spacer installed the dosing of Ca(OH)_2 initially prevents scaling from taking place on the membrane surface, indicating that the dissolve–precipitate effect that the particles exhibit can be used as a precipitative antiscalant for CaCO_3 scaling.

Particulate fouling, however, does take place in other components of the pilot setup, including inside the control valve. The resulting decrease in hydraulic performance caused the cleaning cycle to become less and less effective over time, further worsening the fouling problems until eventually the experiment had to be halted. Therefore, although seemingly effective for a short–term period, the use of Ca(OH)_2 as antiscalant for a longer duration and at different dosages could not be tested.

In the end, however, the problems associated with feed spacers, the necessity of an intermittent cleaning cycle and substantial fouling inside the system make the use of precipitative antis-calants, *for use with conventional spiral-wound polymeric membranes* unattractive compared to more traditional anti-scaling measurements.

Chapter 6

Recommendations

Soft-Sensor for T_{Ca} and T_{CO}

In this thesis the soft-sensor for calculating the total calcium and total carbonate in a solution from the conductivity and pH was only used to determine the dissolution mechanism of calcium hydroxide. Although knowledge on the initial composition of the fluid is required, when the source water is of constant quality, for instance when using groundwater, the sensor may be able to give valuable insight into the performance of other treatment processes.

For instance, the sensor could be used to online monitor the performance of a pellet softening reactor by measuring the EC and pH of the treated water stream, allowing for a more precise control of the lime dosing and split stream ratio. It is therefore recommended to further develop and validate the soft-sensor's performance for other treatment processes.

Kinetics of Slaked Lime Dissolution

The dissolve-precipitate-break-collapse effect that occurs when calcium hydroxide dissolves in water containing carbonate has been observed in previous studies ((Xu et al., 1998; Song and Kim, 1990), and further explored in this thesis. Although the developed soft-sensor helped in forming a hypothetical model of the dissolution mechanisms involved, finding definite proof of the mechanisms occurring falls well outside of the scope of this thesis. It is therefore recommended for more in-depth studies to be done regarding the subject.

In addition, in pellet softeners the breaking and collapsing of the particles may cause issues with part of the softening reaction occurring at unexpected locations in or even outside of the reactor. It is recommended to investigate whether the dissolve-precipitate-break-collapse also takes place in the presence of other surfaces for scale to form on, i.e. pellets.

Precipitative Antiscalants

Due to the problems associated with feed spacers the use of $\text{Ca}(\text{OH})_2$ as precipitative antiscalant is unattractive compared to using traditional antiscalants for polymeric, spiral-wound, membranes. Capillary or ceramic NF membranes, however, have a more optimal hydraulic design and may be less prone to clogging. It is therefore recommended to continue studying $\text{Ca}(\text{OH})_2$ dosing as precipitative antiscalant for those type of membranes.

Furthermore, it is recommended to utilize an installation with more fouling-proof components, such as gate or butterfly valves, so experiments of a longer duration can be conducted.

Bibliography

- Antony, A., Low, J. H., Gray, S., Childress, A. E., Le-Clech, P., and Leslie, G. (2011). Scale formation and control in high pressure membrane water treatment systems: a review. *Journal of Membrane Science*, 383(1):1–16.
- Appelo, C. (2010). Specific conductance: how to calculate, to use, and the pitfalls.
- Apple (2014). *The Swift Programming Language, Swift 2.2 Edition*. Apple Inc.
- Bremere, I., Kennedy, M. D., Johnson, A., Van Emmerik, R., Witkamp, G. J., and Schippers, J. C. (1998). Increasing conversion in membrane filtration systems using a desupersaturation unit to prevent scaling. *Desalination*, 119(1-3):199–204.
- Davies, C. W. (1962). *Ion association*. Butterworths.
- Galan, I., Glasser, F., Baza, D., and Andrade, C. (2015). Assessment of the protective effect of carbonation on portlandite crystals. *Cement and Concrete Research*, 74:68–77.
- Giles, D., Ritchie, I., and Xu, B.-a. (1993). The kinetics of dissolution of slaked lime. *Hydrometallurgy*, 32(1):119–128.
- Hasson, D., Shemer, H., and Sher, A. (2011). State of the art of friendly "green" scale control inhibitors: A review article. *Industrial and Engineering Chemistry Research*, 50(12):7601–7607.
- Hendricks, D. (2010). *Fundamentals of water treatment unit processes: physical, chemical, and biological*. CRC Press.
- Hückel, P. D. E. (1923). The theory of electrolytes. i. lowering of freezing point and related phenomena. *Phys. Z*, 24:185.
- Johannsen, K. and Rademacher, S. (1999). Modelling the kinetics of calcium hydroxide dissolution in water. *Acta Hydrochimica et Hydrobiologica*, 27(2):72–78.
- Kamatani, A., Riley, J. P., and Skirrow, G. (1980). The dissolution of opaline silica of diatom tests in sea water. *Journal of the Oceanographical Society of Japan*, 36(4):201–208.
- Kohlrausch, F. W. G. (1870). *Leitfaden der praktischen Physik: zunächst für das physikalische Prakticum in Göttingen*. Teubner.
- Lin, B., Recke, B., Knudsen, J. K., and Jørgensen, S. B. (2007). A systematic approach for soft sensor development. *Computers & chemical engineering*, 31(5):419–425.
- Moel, P. J. d., Verberk, J., and Van Dijk, J. (2006). *Drinking water: principles and practices*. Singapore: World Scientific.

- Parkhurst, D. L., Thorstenson, D. C., and Plummer, L. N. (1990). Phreeqc—a computer program for geochemical calculations: U.S. Geological Survey water-resources investigations report 80-96. *Revised and reprinted August*, page 195.
- Rahardianto, A., Gao, J., Gabelich, C. J., Williams, M. D., and Cohen, Y. (2007). High recovery membrane desalting of low-salinity brackish water: Integration of accelerated precipitation softening with membrane RO. *Journal of Membrane Science*, 289(1-2):123–137.
- Ritchie, I. M. and Bing-An, X. (1990). The kinetics of lime slaking.
- Song, H. and Kim, C. (1990). The effect of surface carbonation on the hydration of CaO. *Cement and Concrete Research*, 20(5):815–823.
- Stumm, W. and Morgan, J. J. (2012). *Aquatic chemistry: chemical equilibria and rates in natural waters*, volume 126. John Wiley & Sons.
- Sudhakaran, S., Lattemann, S., and Amy, G. L. (2013). Appropriate drinking water treatment processes for organic micropollutants removal based on experimental and model studies: a multi-criteria analysis study. *Science of the Total Environment*, 442:478–488.
- Van de Lisdonk, C., Rietman, B., Heijman, S., Sterk, G., and Schippers, J. (2001). Prediction of supersaturation and monitoring of scaling in reverse osmosis and nanofiltration membrane systems. *Desalination*, 138(1):259–270.
- Van Eekeren, M. and van Paassen, J. (1994). Improved milk-of-lime for softening of drinking water- the answer to the carry-over problem. *Aqua*, 43(1):1–10.
- Verdoes, D. (1996). Water treatment in a Membrane-Assisted Crystallizer (MAC). 104:135–139.
- Vrouwenvelder, J., Manolarakis, S., Veenendaal, H., and van der Kooij, D. (2000). Biofouling potential of chemicals used for scale control in ro and nf membranes. *Desalination*, 132(1-3):1–10.
- Vuik, C., Van Beek, P., Vermolen, F., and Van Kan, J. (2007). *Numerical Methods for Ordinary differential equations*. VSSD.
- Xu, B.-a., Giles, D., and Ritchie, I. (1998). Reactions of lime with carbonate-containing solutions. *Hydrometallurgy*, 48(2):205–224.

Acronyms

AAS	Atomic Absorption Spectrophotometry.....	18
CESP	Chemically Enhanced Seeded Precipitation.....	3
EC	Electrical Conductivity	ix
IC	Ion-Exchange Chromatography	7
MAC	Membrane Assisted Crystallization.....	3
MRC	Membrane Resistance Coefficient.....	x
MF	Micro Filtration	3
NF	Nano Filtration.....	v
OMP	Organic Micro-Pollutant	1
PID	Proportional-Integral-Derivative	32
RO	Reverse Osmosis	1
SI	Saturation Index	14
TMP	Trans Membrane Pressure	1

Appendix A

Analytical Solutions

$$> \text{eq1} := \frac{H \cdot \text{HCO3}}{\text{CO2}} = k1 :$$

$$> \text{eq2} := \frac{H \cdot \text{CO3}}{\text{HCO3}} = k2 :$$

$$> \text{eq3} := \frac{\text{Ca} \cdot \text{CO3}}{\text{CaCO3}} = k3 :$$

$$> \text{eq4} := \frac{\text{Ca} \cdot \text{HCO3}}{\text{CaHCO3}} = k4 :$$

$$> \text{eq5} := \text{TotalCa} = \text{CaCO3} + \text{Ca} + \text{CaHCO3} :$$

$$> \text{eq6} := \text{TotalCO} = \text{CO2} + \text{CO3} + \text{HCO3} + \text{CaCO3} + \text{CaHCO3} :$$

$$> \text{sol} := \text{solve}(\{\text{eq1}, \text{eq2}, \text{eq3}, \text{eq4}, \text{eq5}, \text{eq6}\}, \{\text{CO2}, \text{HCO3}, \text{CO3}, \text{Ca}, \text{CaCO3}, \text{CaHCO3}\}) :$$

$$> \text{assign}(\text{allvalues}(\text{sol})[1 \])$$

> CO2

$$\left(2 \left(-\frac{1}{2} \frac{1}{H^3 k3 + H^2 k1 k3 + H^2 k2 k4 + H k1 k2 k3 + H k1 k2 k4 + k1 k2^2 k4} \left(H^2 (k3 k4 H^2 - H \text{TotalCO} k1 k3 + H \text{TotalCa} k1 k3 + H k1 k3 k4 - \text{TotalCO} k1 k2 k4 + \text{TotalCa} k1 k2 k4 + k1 k2 k3 k4 - (H^4 k3^2 k4^2 + 2 H^3 \text{TotalCO} k1 k3^2 k4 + 2 H^3 \text{TotalCa} k1 k3^2 k4 + 2 H^3 k1 k3^2 k4^2 + H^2 \text{TotalCO}^2 k1^2 k3^2 - 2 H^2 \text{TotalCO} \text{TotalCa} k1^2 k3^2 + 2 H^2 \text{TotalCO} k1^2 k3^2 k4 + 2 H^2 \text{TotalCO} k1 k2 k3 k4^2 + H^2 \text{TotalCa}^2 k1^2 k3^2 + 2 H^2 \text{TotalCa} k1^2 k3^2 k4 + 2 H^2 \text{TotalCa} k1 k2 k3 k4^2 + H^2 k1^2 k3^2 k4^2 + 2 H^2 k1 k2 k3^2 k4^2 + 2 H \text{TotalCO}^2 k1^2 k2 k3 k4 - 4 H \text{TotalCO} \text{TotalCa} k1^2 k2 k3 k4 + 2 H \text{TotalCO} k1^2 k2 k3^2 k4 + 2 H \text{TotalCO} k1^2 k2 k3 k4^2 + 2 H \text{TotalCa}^2 k1^2 k2 k3 k4 + 2 H \text{TotalCa} k1^2 k2 k3^2 k4 + 2 H \text{TotalCa} k1^2 k2 k3 k4^2 + 2 H k1^2 k2 k3^2 k4^2 + \text{TotalCO}^2 k1^2 k2^2 k4^2 - 2 \text{TotalCO} \text{TotalCa} k1^2 k2^2 k4^2 + 2 \text{TotalCO} k1^2 k2^2 k3 k4^2 + \text{TotalCa}^2 k1^2 k2^2 k4^2 + 2 \text{TotalCa} k1^2 k2^2 k3 k4^2 + k1^2 k2^2 k3^2 k4^2)^{1/2} \right) k3 k4 \right) + \frac{1}{2} \frac{1}{H^3 k3 + H^2 k1 k3 + H^2 k2 k4 + H k1 k2 k3 + H k1 k2 k4 + k1 k2^2 k4} \left(H (k3 k4 H^2 - H \text{TotalCO} k1 k3 + H \text{TotalCa} k1 k3 + H k1 k3 k4 - \text{TotalCO} k1 k2 k4 + \text{TotalCa} k1 k2 k4 + k1 k2 k3 k4 - (H^4 k3^2 k4^2 + 2 H^3 \text{TotalCO} k1 k3^2 k4 + 2 H^3 \text{TotalCa} k1 k3^2 k4 + 2 H^3 k1 k3^2 k4^2 + H^2 \text{TotalCO}^2 k1^2 k3^2 - 2 H^2 \text{TotalCO} \text{TotalCa} k1^2 k3^2 + 2 H^2 \text{TotalCO} k1^2 k3^2 k4 + 2 H^2 \text{TotalCO} k1 k2 k3 k4^2 + H^2 \text{TotalCa}^2 k1^2 k3^2 + 2 H^2 \text{TotalCa} k1^2 k3^2 k4 + 2 H^2 \text{TotalCa} k1 k2 k3 k4^2 + H^2 k1^2 k3^2 k4^2 + 2 H^2 k1 k2 k3^2 k4^2 + 2 H \text{TotalCO}^2 k1^2 k2 k3 k4 - 4 H \text{TotalCO} \text{TotalCa} k1^2 k2 k3 k4 + 2 H \text{TotalCO} k1^2 k2 k3^2 k4 + 2 H \text{TotalCO} k1^2 k2 k3 k4^2 + 2 H \text{TotalCa}^2 k1^2 k2 k3 k4 + 2 H \text{TotalCa} k1^2 k2 k3^2 k4 + 2 H \text{TotalCa} k1^2 k2 k3 k4^2 + 2 H k1^2 k2 k3^2 k4^2 + \text{TotalCO}^2 k1^2 k2^2 k4^2 - 2 \text{TotalCO} \text{TotalCa} k1^2 k2^2 k4^2 + 2 \text{TotalCO} k1^2 k2^2 k3 k4^2 + \text{TotalCa}^2 k1^2 k2^2 k4^2 + 2 \text{TotalCa} k1^2 k2^2 k3 k4^2 + k1^2 k2^2 k3^2 k4^2)^{1/2} \right) k3 k4 \right) :$$

Appendix B

Model Source Code

```

//
// model.swift
// InverseModel
//
// Created by Abel Heinsbroek on 05-02-16.
// Copyright © 2016 Mul BV. All rights reserved.
//
import Foundation

func compute(pH:Double, EC:Double, Na: Double, Cl: Double) -> (TCa:Double,TCO:
    Double) {

    // equilibrium constants for activity
    let kwa    = 1.00E-14
    let k1a    = 4.44465E-07
    let k2a    = 4.69052E-11
    let k3a    = 6.03E-04
    let k4a    = 7.84E-02

    // diffusion coefficients
    let DwCa   = 0.793e-9
    let DwNa   = 1.33e-9
    let DwH    = 9.31e-9
    let DwCO3  = 0.955e-9
    let DwOH   = 5.27e-9
    let DwCl   = 2.03e-9
    let DwHCO3 = 1.18e-9
    let DwCaHCO3 = 5.06e-10

    // all the ions in the solution
    var CO2    = 1e-3
    var CO3    = 1e-3
    var HCO3   = 1e-3
    var CaCO3  = 1e-3
    var CaHCO3 = 1e-3
    var H      = 1e-3
    var Ca     = 1e-3

    // equilibrium constants for molality
    var k1     = 1.0
    var k2     = 1.0
    var k3     = 1.0
    var k4     = 1.0
    var kw     = 1.0

    // activity coefficients gamma1 and gamma2
    var gamma1 = 0.9
    var gamma2 = 0.7

    // initial guess ionic strength
    var I      = 1e-2

    // parametric equations to calculate the solution composition, split in
    // substatements to improve performance

    func CalcCO2(TotalCa: Double, TotalCO: Double) -> Double {
        let t1 = H * H; let t2 = k3 * k4; let t4 = TotalCO * H; let t5 = k1 * k3;
        let t7 = H * TotalCa; let t9 = H * k1; let t11 = k1 * TotalCO; let t12
        = k2 * k4; let t14 = k1 * TotalCa; let t16 = k1 * k2; let t18 = t1 *
        t1; let t19 = k3 * k3; let t21 = k4 * k4; let t23 = t1 * H; let t26 =

```

```

k4 * t19 * k1; let t33 = t21 * t19; let t36 = TotalC0 * TotalC0; let
t38 = k1 * k1; let t39 = t19 * t38; let t41 = TotalC0 * t1; let t42 =
t38 * TotalCa; let t46 = k4 * t39; let t50 = k2 * k3; let t51 = t21 *
t50; let t54 = TotalCa * TotalCa; let t57 = TotalCa * t1; let t65 = k1
* t1; let t66 = t19 * k2; let t67 = t21 * t66; let t70 = 2 * t26 *
TotalC0 * t23 + 2 * t26 * TotalCa * t23 + 2 * t33 * k1 * t23 + 2 * t51
* k1 * t41 + 2 * t51 * k1 * t57 + t33 * t38 * t1 + t39 * t36 * t1 +
t39 * t54 * t1 + t21 * t19 * t18 - 2 * t19 * t42 * t41 + 2 * t46 * t41
+ 2 * t46 * t57 + 2 * t67 * t65; let t73 = k4 * t50; let t81 = t38 *
t4; let t82 = k4 * t66; let t91 = t38 * t7; let t100 = k2 * k2; let
t101 = t21 * t100; let t104 = t100 * t38; let t110 = t21 * k3 * t100;
let t118 = -4 * t2 * k2 * t38 * TotalCa * t4 + 2 * t73 * t38 * t36 * H
+ 2 * t73 * t38 * t54 * H - 2 * t21 * t104 * TotalC0 * TotalCa + 2 *
t67 * t38 * H + 2 * t110 * t38 * TotalC0 + t101 * t38 * t36 + t101 *
t38 * t54 + t33 * t104 + 2 * t110 * t42 + 2 * t51 * t81 + 2 * t51 *
t91 + 2 * t82 * t81 + 2 * t82 * t91; let t120 = sqrt(t70 + t118); let
t121 = t1 * t2 - t12 * t11 + t12 * t14 + t2 * t16 + t2 * t9 - t5 * t4
+ t5 * t7 - t120; let t131 = k4 * t100 * k1 + k4 * k2 * t1 + k3 * t23
+ k3 * t65 + t12 * t9 + t50 * t9; let t132 = 0.1e1 / t131; let t138 =
t132 * t121 * H; let t153 = t132 * t121; let t176 = 2 * t131 / t121 /
(t1 + t9 + t16) / k1 / (H * k3 + t12) * t1 * (-k4 * k3 * t132 * t121 *
t1 / 2 + k3 * t11 * t138 / 2 - k3 * t14 * t138 / 2 - k4 * t5 * t138 /
2 + t132 * t121 * k4 * k2 * t11 / 2 - k4 * t16 * TotalCa * t153 / 2 -
t73 * k1 * t153 / 2 - t2 * t11); return t176
}

```

```

func CalcHC03(TotalCa: Double, TotalC0: Double) -> Double {
let t1 = k3 * k4; let t2 = H * H; let t4 = TotalC0 * H; let t5 = k1 * k3;
let t7 = H * TotalCa; let t9 = H * k1; let t12 = k2 * k4; let t18 = t2
* t2; let t19 = k3 * k3; let t21 = k4 * k4; let t23 = t2 * H; let t26
= k4 * t19 * k1; let t33 = t21 * t19; let t36 = TotalC0 * TotalC0; let
t38 = k1 * k1; let t39 = t19 * t38; let t41 = TotalC0 * t2; let t42 =
t38 * TotalCa; let t46 = k4 * t39; let t50 = k2 * k3; let t51 = t21 *
t50; let t54 = TotalCa * TotalCa; let t57 = TotalCa * t2; let t65 = k1
* t2; let t66 = t19 * k2; let t67 = t21 * t66; let t70 = 2 * t26 *
TotalC0 * t23 + 2 * t26 * TotalCa * t23 + 2 * t33 * k1 * t23 + 2 * t51
* k1 * t41 + 2 * t51 * k1 * t57 + t21 * t19 * t18 - 2 * t19 * t42 *
t41 + t33 * t38 * t2 + t39 * t36 * t2 + t39 * t54 * t2 + 2 * t46 * t41
+ 2 * t46 * t57 + 2 * t67 * t65; let t73 = k4 * t50; let t81 = t38 *
t4; let t82 = k4 * t66; let t91 = t38 * t7; let t100 = k2 * k2; let
t101 = t21 * t100; let t104 = t100 * t38; let t110 = t21 * k3 * t100;
let t118 = -4 * t1 * k2 * t38 * TotalCa * t4 + 2 * t73 * t38 * t36 * H
+ 2 * t73 * t38 * t54 * H - 2 * t21 * t104 * TotalC0 * TotalCa + 2 *
t67 * t38 * H + 2 * t110 * t38 * TotalC0 + t101 * t38 * t36 + t101 *
t38 * t54 + t33 * t104 + 2 * t110 * t42 + 2 * t51 * t81 + 2 * t51 *
t91 + 2 * t82 * t81 + 2 * t82 * t91; let t120 = sqrt(t70 + t118); let
t135 = -H / (k4 * t100 * k1 + k4 * k2 * t2 + k3 * t23 + k3 * t65 + t12
* t9 + t50 * t9) * (-t12 * TotalC0 * k1 + t12 * TotalCa * k1 + t1 * k1
* k2 + t1 * t2 + t1 * t9 - t5 * t4 + t5 * t7 - t120) / 2;
return t135
}

```

```

func CalcC03(TotalCa: Double, TotalC0: Double) -> Double {
let t1 = k3 * k4; let t2 = H * H; let t4 = TotalC0 * H; let t5 = k1 * k3;
let t7 = H * TotalCa; let t9 = H * k1; let t12 = k2 * k4; let t18 = t2
* t2; let t19 = k3 * k3; let t21 = k4 * k4; let t23 = t2 * H; let t26
= k4 * t19 * k1; let t33 = t21 * t19; let t36 = TotalC0 * TotalC0; let
t38 = k1 * k1; let t39 = t19 * t38; let t41 = TotalC0 * t2; let t42 =
t38 * TotalCa; let t46 = k4 * t39; let t50 = k2 * k3; let t51 = t21 *
t50; let t54 = TotalCa * TotalCa; let t57 = TotalCa * t2; let t65 = k1

```

```

* t2; let t66 = t19 * k2; let t67 = t21 * t66; let t70 = 2 * t26 *
TotalC0 * t23 + 2 * t26 * TotalCa * t23 + 2 * t33 * k1 * t23 + 2 * t51
* k1 * t41 + 2 * t51 * k1 * t57 + t21 * t19 * t18 - 2 * t19 * t42 *
t41 + t33 * t38 * t2 + t39 * t36 * t2 + t39 * t54 * t2 + 2 * t46 * t41
+ 2 * t46 * t57 + 2 * t67 * t65; let t73 = k4 * t50; let t81 = t38 *
t4; let t82 = k4 * t66; let t91 = t38 * t7; let t100 = k2 * k2; let
t101 = t21 * t100; let t104 = t100 * t38; let t110 = t21 * k3 * t100;
let t118 = -4 * t1 * k2 * t38 * TotalCa * t4 + 2 * t73 * t38 * t36 * H
+ 2 * t73 * t38 * t54 * H - 2 * t21 * t104 * TotalC0 * TotalCa + 2 *
t67 * t38 * H + 2 * t110 * t38 * TotalC0 + t101 * t38 * t36 + t101 *
t38 * t54 + t33 * t104 + 2 * t110 * t42 + 2 * t51 * t81 + 2 * t51 *
t91 + 2 * t82 * t81 + 2 * t82 * t91; let t120 = sqrt(t70 + t118); let
t135 = -1 / (k4 * t100 * k1 + k4 * k2 * t2 + k3 * t23 + k3 * t65 + t12
* t9 + t50 * t9) * (-t12 * TotalC0 * k1 + t12 * TotalCa * k1 + t1 * k1
* k2 + t1 * t2 + t1 * t9 - t5 * t4 + t5 * t7 - t120) * k2 / 2; return
t135 }

func CalcCa(TotalCa: Double, TotalC0: Double) -> Double {
    let t1 = H * H; let t2 = k4 * k3; let t4 = H * TotalC0; let t5 = k1 * k3;
    let t7 = H * TotalCa; let t9 = H * k1; let t11 = k1 * TotalC0; let t12
    = k2 * k4; let t16 = k1 * k2; let t18 = t1 * t1; let t19 = k3 * k3;
    let t21 = k4 * k4; let t23 = t1 * H; let t26 = k4 * t19 * k1; let t33
    = t21 * t19; let t36 = TotalC0 * TotalC0; let t38 = k1 * k1; let t39 =
    t19 * t38; let t41 = TotalC0 * t1; let t42 = t38 * TotalCa; let t46 =
    k4 * t39; let t50 = k3 * k2; let t51 = t21 * t50; let t54 = TotalCa *
    TotalCa; let t57 = TotalCa * t1; let t65 = k1 * t1; let t66 = t19 *
    k2; let t67 = t21 * t66; let t70 = 2 * t26 * TotalC0 * t23 + 2 * t26 *
    TotalCa * t23 + 2 * t33 * k1 * t23 + 2 * t51 * k1 * t41 + 2 * t51 * k1
    * t57 + t33 * t38 * t1 + t39 * t36 * t1 + t39 * t54 * t1 + t21 * t19 *
    t18 - 2 * t19 * t42 * t41 + 2 * t46 * t41 + 2 * t46 * t57 + 2 * t67 *
    t65; let t73 = k4 * t50; let t81 = t38 * t4; let t82 = k4 * t66; let
    t91 = t38 * t7; let t100 = k2 * k2; let t101 = t21 * t100; let t104 =
    t100 * t38; let t110 = t21 * k3 * t100; let t118 = -4 * t2 * k2 * t38
    * TotalCa * t4 + 2 * t73 * t38 * t36 * H + 2 * t73 * t38 * t54 * H - 2
    * t21 * t104 * TotalC0 * TotalCa + 2 * t67 * t38 * H + 2 * t110 * t38
    * TotalC0 + t101 * t38 * t36 + t101 * t38 * t54 + t33 * t104 + 2 *
    t110 * t42 + 2 * t51 * t81 + 2 * t51 * t91 + 2 * t82 * t81 + 2 * t82 *
    t91; let t120 = sqrt(t70 + t118); let t121 = t12 * TotalCa * k1 + t1 *
    t2 - t12 * t11 + t2 * t16 + t2 * t9 - t5 * t4 + t5 * t7 - t120; let
    t131 = k4 * t100 * k1 + k4 * k2 * t1 + k3 * t23 + k3 * t65 + t12 * t9
    + t50 * t9; let t132 = 1 / t131; let t154 = 2 * t131 / t121 / k1 / (H
    * k3 + t12) * k4 * k3 * (-t132 * t121 * t1 / 2 - k1 * t132 * t121 *
    H / 2 - t16 * t132 * t121 / 2 - t11);
    return t154
}

func CalcCaC03(TotalCa: Double, TotalC0: Double) -> Double {
    let t1 = k2 * k4; let t2 = H * H; let t3 = k4 * k3; let t5 = H * TotalC0;
    let t6 = k1 * k3; let t8 = H * TotalCa; let t10 = H * k1; let t12 = k1
    * TotalC0; let t14 = TotalCa * k1; let t16 = k1 * k2; let t18 = t2 *
    t2; let t19 = k3 * k3; let t21 = k4 * k4; let t23 = t2 * H; let t26 =
    k4 * t19 * k1; let t33 = t21 * t19; let t36 = TotalC0 * TotalC0; let
    t38 = k1 * k1; let t39 = t19 * t38; let t41 = TotalC0 * t2; let t42 =
    t38 * TotalCa; let t46 = k4 * t39; let t50 = k3 * k2; let t51 = t21 *
    t50; let t54 = TotalCa * TotalCa; let t57 = TotalCa * t2; let t65 = k1
    * t2; let t66 = t19 * k2; let t67 = t21 * t66; let t70 = 2 * t26 *
    TotalC0 * t23 + 2 * t26 * TotalCa * t23 + 2 * t33 * k1 * t23 + 2 * t51
    * k1 * t41 + 2 * t51 * k1 * t57 + t21 * t19 * t18 - 2 * t19 * t42 *
    t41 + t33 * t38 * t2 + t39 * t36 * t2 + t39 * t54 * t2 + 2 * t46 * t41
    + 2 * t46 * t57 + 2 * t67 * t65; let t73 = k4 * t50; let t81 = t38 *

```

```

t5; let t82 = k4 * t66; let t91 = t38 * t8; let t100 = k2 * k2; let
t101 = t21 * t100; let t104 = t100 * t38; let t110 = t21 * k3 * t100;
let t118 = -4 * t3 * k2 * t38 * TotalCa * t5 + 2 * t73 * t38 * t36 * H
+ 2 * t73 * t38 * t54 * H - 2 * t21 * t104 * TotalCO * TotalCa + 2 *
t67 * t38 * H + 2 * t110 * t38 * TotalCO + t101 * t38 * t36 + t101 *
t38 * t54 + t33 * t104 + 2 * t110 * t42 + 2 * t51 * t81 + 2 * t51 *
t91 + 2 * t82 * t81 + 2 * t82 * t91; let t120 = sqrt(t70 + t118); let
t121 = -t1 * t12 + t1 * t14 + t3 * t10 + t3 * t16 + t2 * t3 - t6 * t5
+ t6 * t8 - t120; let t131 = k4 * t100 * k1 + k4 * k2 * t2 + k3 * t23
+ k3 * t65 + t1 * t10 + t50 * t10; let t132 = 0.1e1 / t131; let t138 =
t132 * t121 * H; let t145 = t132 * t121; let t158 = pow(H * k3 + t1,
2); let t167 = -2 * t131 / t121 / k1 / t158 * (-k4 * k3 * t132 * t121
* t2 / 2 - k3 * t14 * t138 / 2 - k4 * t6 * t138 / 2 - k4 * t16 *
TotalCa * t145 / 2 - t73 * k1 * t145 / 2 - t3 * t12) * t1;
return t167
}

```

```

func CalcCaHC03(TotalCa: Double, TotalCO: Double) -> Double {
let t1 = H * k3; let t2 = H * H; let t3 = k4 * k3; let t5 = H * TotalCO;
let t6 = k1 * k3; let t8 = H * TotalCa; let t10 = H * k1; let t12 = k1
* TotalCO; let t13 = k2 * k4; let t17 = k1 * k2; let t19 = t2 * t2;
let t20 = k3 * k3; let t22 = k4 * k4; let t24 = t2 * H; let t27 = k4 *
t20 * k1; let t34 = t22 * t20; let t37 = TotalCO * TotalCO; let t39 =
k1 * k1; let t40 = t20 * t39; let t42 = TotalCO * t2; let t43 = t39 *
TotalCa; let t47 = k4 * t40; let t51 = k3 * k2; let t52 = t22 * t51;
let t55 = TotalCa * TotalCa; let t58 = TotalCa * t2; let t66 = k1 *
t2; let t67 = t20 * k2; let t68 = t22 * t67; let t71 = 2 * t27 *
TotalCO * t24 + 2 * t27 * TotalCa * t24 + 2 * t34 * k1 * t24 + 2 * t52
* k1 * t42 + 2 * t52 * k1 * t58 + t22 * t20 * t19 + t34 * t39 * t2 +
t40 * t37 * t2 + t40 * t55 * t2 - 2 * t20 * t43 * t42 + 2 * t47 * t42
+ 2 * t47 * t58 + 2 * t68 * t66; let t74 = k4 * t51; let t82 = t39 *
t5; let t83 = k4 * t67; let t92 = t39 * t8; let t101 = k2 * k2; let
t102 = t22 * t101; let t105 = t101 * t39; let t111 = t22 * k3 * t101;
let t119 = -4 * t3 * k2 * t39 * TotalCa * t5 + 2 * t74 * t39 * t37 * H
+ 2 * t74 * t39 * t55 * H - 2 * t22 * t105 * TotalCO * TotalCa + 2 *
t68 * t39 * H + 2 * t111 * t39 * TotalCO + t102 * t39 * t37 + t102 *
t39 * t55 + t34 * t105 + 2 * t111 * t43 + 2 * t52 * t82 + 2 * t52 *
t92 + 2 * t83 * t82 + 2 * t83 * t92; let t121 = sqrt(t71 + t119); let
t122 = t13 * TotalCa * k1 + t3 * t10 - t13 * t12 + t3 * t17 + t2 * t3
- t6 * t5 + t6 * t8 - t121; let t133 = 1 / (k4 * t101 * k1 + k4 * k2 *
t2 + k3 * t24 + k3 * t66 + t13 * t10 + t51 * t10); let t150 = -1 /
k1 / (t1 + t13) * (-t133 * t122 * t2 / 2 - k1 * t133 * t122 * H / 2 -
t17 * t133 * t122 / 2 - t12) * t1;
return t150
}

```

```

// calculate ionic strength

```

```

func CalcI() {
I = 0.5*(CO3*4+Ca*4+HC03+kw/H+Na+Cl+CaHC03)
}

```

```

// calculate gamma1 and gamma2 from the ionic strength

```

```

func CalcGamma() {
gamma1 = pow(10, (-0.5*(((sqrt(I))/(1+sqrt(I)))-0.3*I)))
gamma2 = pow(10, (-2*(((sqrt(I))/(1+sqrt(I)))-0.3*I)))

kw = kwa/(gamma1*gamma1)
k1 = k1a/(gamma1*gamma1)
k2 = k2a/(gamma2)
k3 = k3a/(gamma2*gamma2)
}

```

```

    k4 = k4a/gamma2
}

// calculate the specific conductivity of an ion
func SC(m:Double,z:Double,dw:Double,gamma:Double) -> Double {
    let F = 96493.5 // Faradays Constant
    let R = 8.3144598 // Gas Constant
    let T = 298.160 // Absolute temperature
    let SC = (pow(gamma,0.6/sqrt(z))*m*pow(z,2)*dw*pow(F,2))/(R*T)*1e7
    return SC
}

// calculate solution composition
func CalcMolality(TotalCO: Double,TotalCa: Double){
    CO2 = CalcCO2(TotalCa,TotalCO: TotalCO)
    HCO3 = CalcHCO3(TotalCa,TotalCO: TotalCO)
    CO3 = CalcCO3(TotalCa,TotalCO: TotalCO)
    CO2 = CalcCO2(TotalCa,TotalCO: TotalCO)
    Ca = CalcCa(TotalCa,TotalCO: TotalCO)
    CaCO3 = CalcCaCO3(TotalCa,TotalCO: TotalCO)
    CaHCO3 = CalcCaHCO3(TotalCa,TotalCO: TotalCO)
}

// root function 1 (on conductivity)
func eq1(TotalCO: Double, TotalCa: Double) -> Double {
    CalcMolality(TotalCO, TotalCa: TotalCa)
    let e1 = EC - SC(Ca,z: 2,dw: DwCa,gamma: gamma2) - SC(kw/H,z: 1,dw: DwOH,
        gamma: gamma1) - SC(CO3,z: 2,dw: DwCO3,gamma: gamma2)
    let e2 = SC(HCO3,z: 1,dw: DwHCO3,gamma: gamma1) + SC(Cl,z: 1,dw: DwCl,
        gamma: gamma1) + SC(Na,z: 1,dw: DwNa,gamma: gamma1) + SC(CaHCO3,z:
        1,dw:DwCaHCO3,gamma: gamma2)
    return e1-e2
}

// root function 2 (on charge)
func eq2(TotalCO: Double, TotalCa: Double) -> Double {
    CalcMolality(TotalCO,TotalCa: TotalCa)
    let error = (H+2*Ca-HCO3-kw/H-2*CO3+CaHCO3)
    return error
}

// set initial values for gamma1 and gamma2 based on the guess for ionic
// strength
CalcGamma()

// calculate H+ from the pH
H = pow(10,-pH)/gamma1

// initial guess for total carbonate
var TCO = 1e-3
// initial guess for total calcium
var TCa = 1e-3

// Newton-Rhapson implementation
for _ in 0..<20 {
    let nstep = 1e-8
    // numerical differeniation
    let eq11 = (eq1(TCO+nstep,TotalCa: TCa)-eq1(TCO,TotalCa: TCa))/nstep
    let eq12 = (eq1(TCO,TotalCa: TCa+nstep)-eq1(TCO,TotalCa: TCa))/nstep
    let eq21 = (eq2(TCO+nstep,TotalCa: TCa)-eq2(TCO,TotalCa: TCa))/nstep
}

```

```

let eq22 = (eq2(TCO,TotalCa: TCa+nstep)-eq2(TCO,TotalCa: TCa))/nstep

// assemble inverse jacobian
let invm = 1/(eq11*eq22-eq12*eq21)
let J11 = invm*eq22
let J12 = -invm*eq12
let J21 = -invm*eq21
let J22 = invm*eq11

// calculate residuals
let v1 = eq1(TCO,TotalCa: TCa)
let v2 = eq2(TCO,TotalCa: TCa)

// calculate product vector
let p1 = J11*v1 + J12*v2
let p2 = J21*v1 + J22*v2

// update guess
TCO -= p1
TCa -= p2

// recalculate ionic strength and activity coefficients
CalcI()
CalcGamma()

// update molality of H+ ions
H = pow(10,-pH)/gamma1
}
return (TCa,TCO)
}

var ecData = [Double]()
var pHData = [Double]()
var Na = 5e-3
var Cl = 5e-3

// read input from command line
for arg in Process.arguments {
  let varg = arg.componentsSeparatedByString("=")
  switch(varg[0]) {
  case "--EC":
    let data = varg[1].componentsSeparatedByString(",")
    print("EC")
    for point in data {
      ecData.append(Double(point)!)
    }
  case "--pH":
    let data = varg[1].componentsSeparatedByString(",")
    print("pH")
    for point in data {
      pHData.append(Double(point)!)
    }
  case "--Na":
    print("Na")
    Na = Double(varg[1])!
  case "--Cl":
    print("Cl")
    Cl = Double(varg[1])!
  }
}

```

```
    default:
        let a = 1
        // do notnithg
    }
}

var output=""

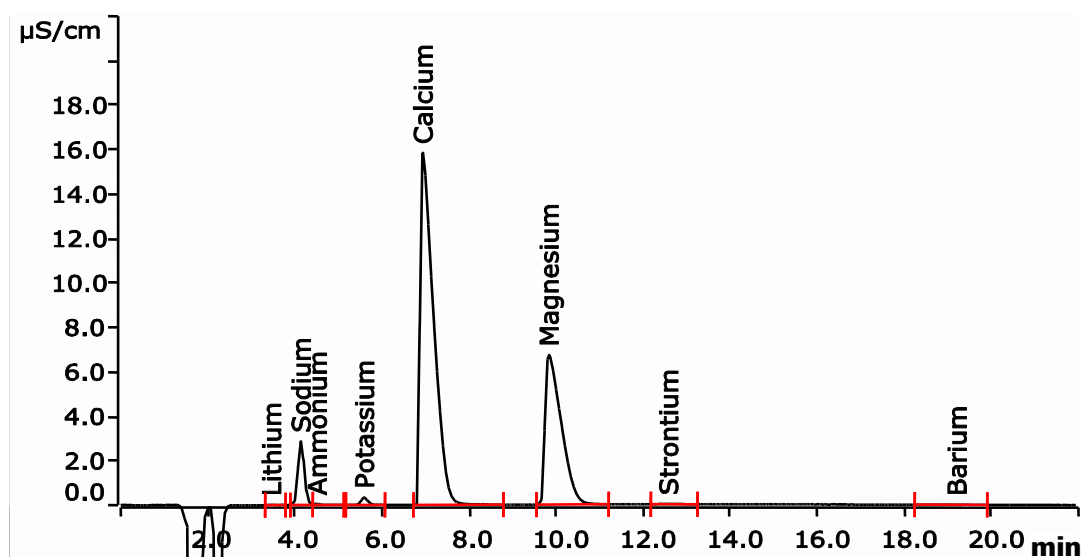
let iter = min(ecData.count,pHData.count)

// run the program, use Grand Central Dispatch to parallelize computation.
for i in 0..
```


Appendix C

Calcium IC Measurement Procedure

Cations in drinking water using Metrosep C 4 - 150/4.0 column according to ISO 14911



Drinking water analysis is strongly regulated by standards. In this Application Note, the cation determination according to ISO 14911 is shown. The Metrosep C 4 - 150/4.0 is the optimum separation column for this purpose.

Results

Cation	[mg/L]	RSD (% , n = 3)
Lithium	< 0.01	
Sodium	5.33	0.5
Ammonium	0.07	3.1
Potassium	0.24	1.0
Calcium	85.30	0.5
Magnesium	18.52	0.6
Strontium	0.22	5.0
Barium	< 0.10	

Method description

Sample

Drinking water

Sample preparation

Metrohm intelligent Partial Loop Technique (MiPT)

Column

Metrosep C 4 - 150/4.0	6.1050.420
Metrosep C 4 Guard/4.0	6.1050.500

Solutions

Eluent	2.0 mmol/L nitric acid 2.0 mmol/L dipicolinic acid
--------	---

Analysis

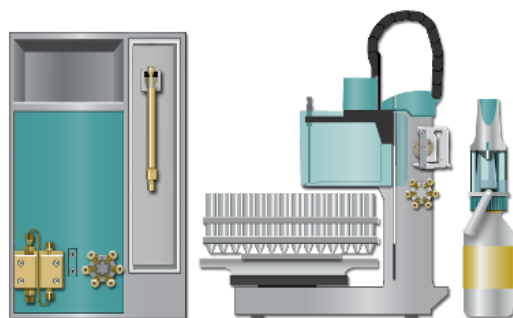
Non-suppressed conductivity

Parameters

Flow rate	0.9 mL/min
Injection volume	10 μ L
P _{max}	15.0 MPa
Recording time	20 min
Column temperature	30 °C

Instrumentation

881 Compact IC pro	2.881.0010
858 Professional Sample Processor	2.858.0010
800 Dosino	2.800.0010



www.metrohm.com

 **Metrohm**

Appendix D

Carbonate IC Measurement Procedure

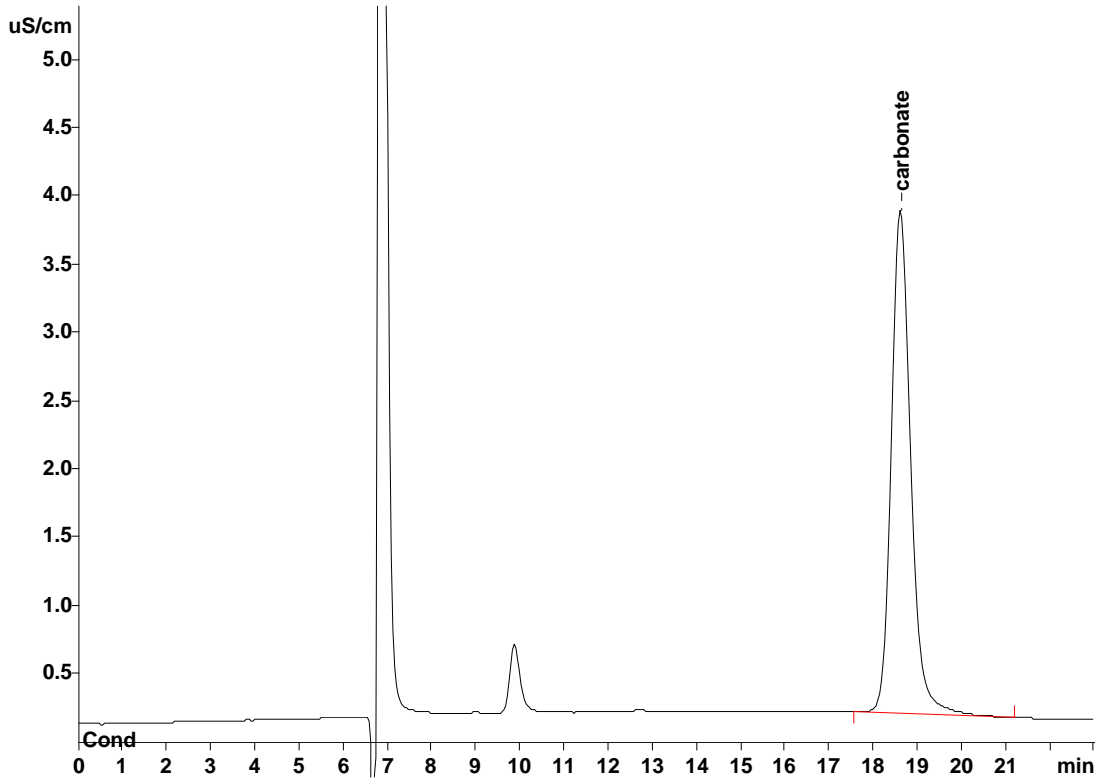
IC Application Note No. O-30

Title: Carbonate in tap water using ion exclusion chromatography

Summary: Determination of carbonate in tap water using ion exclusion chromatography with suppressed conductivity detection.

Sample: Tap water from Houston
Sample Preparation: –

Column: 6.1005.200 Metrosep Organic Acids
Eluent: 0.5 mmol/L sulfuric acid
Flow: 0.5 mL/min
Suppressor: MSM (25 mmol/L lithium chloride)
Injection Volume: 20 μ L



Results:	Carbonate mg/L
	104.3

Appendix E

Flat Sheet Membrane Specifications



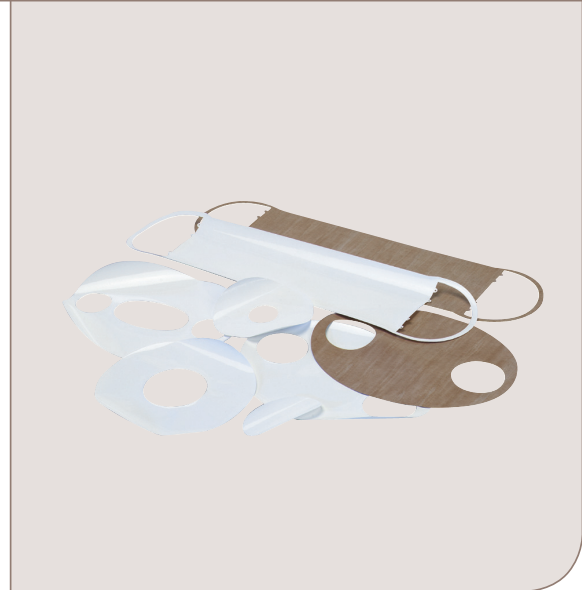
Flat Sheet Membranes

Nanofiltration and Reverse Osmosis Membranes

The range of nanofiltration and reverse osmosis membranes from Alfa Laval covers a broad spectrum of flux and rejection properties. The membranes are based on a unique construction of either polypropylene (PP) or polyester (PE) support material that provides optimum cleaning conditions

Alfa Laval flat sheet membranes are available by the metre, as standard sheets (size 20 x 20 cm), and of course in all Alfa Laval plate-and-frame configurations. All the materials used for the production of these membranes comply with FDA regulations (CFR) Title 21.

All Alfa Laval flat sheet membranes will be delivered with necessary lock and passage rings.



Designation	Characteristics	Rejection
Polyester support		
RO99	Thinfil composite	> 98%*
RO90	Thinfil composite	> 90%**
NF	Thinfil composite	> 98%***
Polypropylene support		
RO98pHt	Thinfil composite	> 97%*

* measured on 2000 ppm NaCl, 16 bar, 25°C

** measured on 2000 ppm NaCl, 9 bar, 25°C

*** measured on 2000 ppm MgSO₄, 9 bar, 25°C

Standard dimensions and part numbers

Membrane type	Standard sheets 20 x 20 cm	Alfa Laval Module M20	Alfa Laval Module M30
RO90	525517	525516	525518
RO99	522386	522369	524288
RO98pHt	100316	100457	100600
NF	517819	517820	517732

Other flat sheet sizes may be available - please contact Alfa Laval.

Recommended operation limits

Production

	RO99 / RO90	NF	RO98pHt
pH range	3-10	3-10	2-11
Typical operating pressure, bar	15-42	15-42	15-42
Maximum operating pressure, bar	55	55	55
Temperature, °C	5-50	5-50	5-60

Cleaning (3 hours per day)*

	RO99 / RO90	NF	RO98pHt
Pressure, bar	1-5	1-5	1-5
Temperature, °C	30-50 (86-122)	30-50	30-60
pH range	1.5-11.0	1.5-11.0	1.5-12.5
NaOH, %	<0.1	<0.1	<0.3
Na-EDTA, %	<0.2	<0.2	<0.2
Mineral acid, %	<0.2	<0.2	<0.2
Citric acid, %	<1.0	<1.0	<1.0

Note: The use of oxidation agents and similar chemicals might influence the actual membrane performance over time and agents such as chlorine are not allowed.

Sanitation (1 hour per week)

	RO99 / RO90	NF	RO98pHt
Hydrogen peroxide (ppm) at 25°C	<1,000	<1,000	<1,000

* Please consult the Alfa Laval "Water quality" PD leaflet, 1603.

Important information

New membranes must be cleaned prior to first use. The cleaning procedure should be in accordance with the instructions provided in the Alfa Laval cleaning description for the membrane type concerned. The customer is fully responsible for the effects that any incompatible chemicals may have on the membranes.

- After initial wetting, the membranes must be kept moist at all times.
- If the operating specifications provided in this product description are not strictly followed, the limited warranty will be null and void.
- To prevent biological growth during system shutdowns, Alfa Laval recommends that membranes should be immersed in a protective solution.
- Avoid permeate-side back pressure at all times.

Operation guidelines

Avoid any abrupt pressure or cross-flow variations on the membranes during startup, shutdown, cleaning or other sequences, in order to prevent possible damage.

Alfa Laval recommends the following start-up procedure from standstill to operating condition:

- The unpressurized plant should be refilled with water.
- Feed pressure should be gradually increased over a 30–60 second time scale.
- Before initiating cross-flow at high permeate flux conditions (e.g. start-up with high-temperature water), the set feed pressure should be maintained for 5–10 minutes.
- Cross-flow velocity at the set operating point should be gradually achieved over a period of 15–20 seconds.
- Temperature variations should be implemented gradually over a period of 3–5 minutes.

Alfa Laval reserves the right to change specifications without prior notification. ALFA LAVAL is a trademark registered and owned by Alfa Laval Corporate AB.

How to contact Alfa Laval

Contact details for all countries are continually updated on our website. Please visit www.alfalaval.com to access the information direct.